Complementary regulation of TBC1D1 and AS160 by growth factors, insulin and AMPK activators

Shuai Chen, Jane Murphy, Rachel Toth, David G Campbell, Nick A Morrice, Carol Mackintosh

Complementary regulation of TBC1D1 and AS160 by growth factors, insulin and AMPK activators

Shuai Chen, Jane Murphy, Rachel Toth, David G. Campbell, Nick A. Morrice, and Carol MacKintosh

MRC Protein Phosphorylation Unit, College of Life Sciences, University of Dundee, Dundee DD1 5EH, Scotland, U.K.

Running title: Phosphorylation and 14-3-3 binding of TBC1D1

Keywords: 14-3-3, PKB, AMPK, AS160, obesity, TBC1D1, metformin

Correspondence to: Carol MacKintosh

Tel: 44-1382-344241

FAX: 44-1382-223778

E-mail: c.mackintosh@dundee.ac.uk

Abbreviations:

AICAR, 5-aminoimidazole-4-carboxamide-1-ß-D-ribofuranoside; AS160, Akt substrate of 160 kDa (also known as TBC1D4); DSP, dithiobis[succinimidyl propionate]; ERK, extracellular-signal-regulated protein kinase; GAP, GTPase-activating protein; GST, glutathione S-transferase; GSV, GLUT4 storage vesicle; HA, haemagglutinin; IGF1, insulin-like growth factor-1; MS, mass spectrometry; MS/MS, tandem mass spectrometry; PI 3-kinase, phosphatidylinositide 3-kinase; PKB, protein kinase B (also known as Akt); PTB, phosphotyrosine binding domain; RSK, p90 ribosomal S6 kinase; TBC1D1, tre-2/USP6, BUB2, cdc16 domain family member 1 (the TBC domain is the GAP domain).

ABSTRACT

AS160 and TBC1D1 are related RabGAPs implicated in regulating the trafficking of GLUT4 storage vesicles to the cell surface. All animal species examined contain TBC1D1, whereas AS160 evolved with the vertebrates. TBC1D1 has two clusters of phosphorylated residues, either side of the second PTB domain. Each cluster contains a 14-3-3-binding site. When AMPK is activated in HEK293 cells, 14-3-3s bind primarily to phosphoSer237 in TBC1D1; whereas 14-3-3 binding depends primarily on phosphoThr596 in cells stimulated with insulin-like growth factor 1 (IGF1), epidermal growth factor (EGF) and phorbol ester (PMA); and both phosphoSer237 and phosphoThr596 contribute to 14-3-3 binding in cells stimulated with forskolin. In HEK293 cells, LY294002 inhibits phosphorylation of Thr596 of TBC1D1, and promotes phosphorylation of AMPK and Ser237 of TBC1D1. In vitro phosphorylation experiments indicated regulatory interactions amongst phosphorylated sites, for example phosphorylation of Ser235 prevents subsequent phosphorylation of Ser237. In rat L6 myotubes, endogenous TBC1D1 is strongly phosphorylated on Ser237 and binds to 14-3-3s in response to the AMPK activators AICAR, phenformin and A-769662, whereas insulin promotes phosphorylation of Thr596 but not 14-3-3 binding. In contrast, AS160 is phosphorylated on its 14-3-3-binding sites (Ser341 and Thr642) and binds to 14-3-3s in response to insulin, but not A-769662, in L6 cells. These findings suggest that TBC1D1 and AS160 may have complementary roles in regulating vesicle trafficking in response to insulin and AMPK-activating stimuli in skeletal muscle.

INTRODUCTION

Rabs are GTP-activated proteins that regulate the flow of vesicle traffic between organelles by interacting with effectors of vesicle formation, motility, docking and fusion [1]. Inactive GDP-Rabs are held by Rab GDP dissociation inhibitors (GDIs), and upon release guanine nucleotide exchange factors (GEFs) convert GDP-Rabs to the active GTP-Rabs. GTPase activating proteins (GAPs) inactivate Rabs by enhancing their intrinsic GTP-hydrolysing activities [2].

AS160/TBC1D4 and TBC1D1 are related RabGAPs implicated in regulating translocation of GLUT4 glucose transporters from intracellular GLUT4 storage vesicles (GSVs) to the plasma membrane [3,4]. It has been proposed that AS160 and/or TBC1D1 must be inhibited for GSV-bound Rabs to stay loaded with GTP so that GLUT4 can move to the cell surface and import glucose into cells in response to stimuli such as insulin and exercise [5,6]. The tissue distribution of AS160 and TBC1D1 is wider than GLUT4 however [7,8], suggesting that these RabGAPs also regulate trafficking of vesicles containing other unknown cargoes.

The mechanisms of control of AS160 are being defined: At least eight residues are phosphorylated in response to insulin, insulin-like growth factor 1 (IGF1), epidermal growth factor (EGF), the phorbol ester PMA, and AMPK activator AICAR, though the extents of phosphorylation of different sites vary with each stimulus [3, 9, 10]. In IGF1-, EGF-, and PMA-stimulated cells 14-3-3 proteins have been found to bind with high affinity to phosphoThr642 on AS160, while phosphoSer341 provides a secondary 14-3-3-binding site [10,11]. These findings suggest the hypothesis that a single 14-3-3 dimer docks onto phosphoThr642 and phosphoSer341, thereby affecting the function of the PTB domain, which is located between these two residues. Ectopic expression of non-phosphorylatable forms of AS160 that cannot bind to 14-3-3s is sufficient to impair insulin-stimulated glucose uptake into cells [11,12], consistent with the possibility that phosphorylation and 14-3-3 binding across the PTB domain inhibits AS160.

The signatures of AS160 phosphorylation by protein kinases in vitro, and effects of protein kinase inhibitors in cells, are consistent with Thr642 of AS160 being phosphorylated by PKB in response to IGF1, and Ser341 and Thr642 being phosphorylated by RSK in response to PMA. However, the kinase that mediates phosphorylation of Ser341 in response to IGF1 is unknown [10]. Ser588 is strongly phosphorylated by AMPK in vitro and in response to the

AMPK activator AICAR in cells. However, the more potent AMPK activator phenformin does not promote AS160 phosphorylation. Thus, it is possible that an AICAR-activated kinase other than AMPK phosphorylates Ser588 in vivo [10].

Less is known about TBC1D1, except that a mutation in TBC1D1 has been linked with a strong familial predisposition to severe obesity in females [8, 13, 14], and TBC1D1 is similar to AS160 with respect to its specificity towards Rabs in vitro, phosphorylation on a Thr residue (Thr596, within a potential PKB recognition sequence) in response to insulin, and wide tissue distribution [4]. One distinction between AS160 and TBC1D1 is that ectopic expression of wild-type TBC1D1 inhibits GLUT4 translocation, whereas only non-phosphorylatable forms of AS160 have this effect [4].

Stemming from the identification of TBC1D1 amongst proteins isolated from HEK293 cell extracts by 14-3-3-affinity purification [15], here we investigate its regulation. We find similarities, but also striking differences, in the patterns of phosphorylation and 14-3-3-binding of TBC1D1, compared to what is known about AS160. Our findings give new insights into how clusters of multisite phosphorylation may modulate 14-3-3 binding to target sites.

MATERIALS AND METHODS

Materials

Synthetic peptides were from Graham Bloomberg (Department of Biochemistry, University of Bristol), oligonucleotides from MWG-Biotech, IGF1 (insulin-like growth factor 1) from Biosource, microcystin-LR from Linda Lawton (School of Life Sciences, The Robert Gordon University, Aberdeen), Vivaspin concentrators from Vivascience, tissue culture reagents and epidermal growth factor from Life Technologies, protease-inhibitor cocktail tablets (no. 1697498) and sequencing grade trypsin from Roche Molecular Biochemicals, 5-aminoimidazole-4-carboxamide-1-beta-D-ribofuranoside (AICAR) from Toronto Research Chemicals (North York, ON, Canada), 6-[4-(2-Piperidin-1-yl-ethoxy)-phenyl)]-3-pyridin-4-yl-pyrrazolo[1,5-a]-pyrimidine (Compound C), A23187 and calyculin A from Calbiochem, metformin, phenformin and PMA from Sigma-Aldrich, insulin from Novo-Nordisk, BI-D1870 from Boehringer Ingelheim Pharma GmbH & Co., precast SDS–polyacrylamide gels from Invitrogen, and dithiobis[succinimidyl propionate] (DSP) from Perbio. Protein G-Sepharose and other chromatographic matrices were from GE-Healthcare. All other chemicals were from

BDH Chemicals or Sigma-Aldrich.

Antibodies and protein kinases

Anti-HA was raised in sheep against the synthetic peptide YPYDVPDYA. The antibodies that recognise phosphorylated sites in TBC1D1 were raised against the following synthetic phosphopeptides:- CPMRKSFpSQPGLRS (Cys for coupling, plus residues 231 to 243 of human TBC1D1, where pS represents phosphorylated Ser237) and CFRRRANpTLSHFPI (Cys + 590 to 602 of human TBC1D1, pT is phosphorylated Thr596). The peptides were conjugated via the added cysteines to BSA and keyhole-limpet haemocyanin and injected into sheep at Diagnostics Scotland (Penicuik, UK). The antibodies were affinity-purified on CH-Sepharose coupled to the same peptide. Sheep antibodies for immunoprecipitating TBC1D1 were raised against a GST-TBC1D1-C-terminal fragment (residues 640 to 1168) that was expressed in *E. coli* and purified, and antibodies used for immunocytochemistry were raised against full-length GST-TBC1D1. Phospho-specific antibodies for sites in AS160 were reported in [10]. The pan-14-3-3 antibody was K19 from Santa Cruz; the antibodies that recognise phosphorylated Thr172 on AMPK and phosphorylated Thr308 on PKB, anti-phospho (Ser/Thr)-Akt/PKB substrate (PAS) antibody, and anti-Erk1/2 antibody were from Cell Signaling Technology; and the antibody that recognises phosphorylated Ser80 on human acetyl-CoA carboxylase (ACC) (pSer79 on the rat protein) and anti-AS160 were from Millipore.

Purified recombinant protein kinases, generated in the Division of Signal Tranduction Therapy (DSTT), were His-PKBalpha-S473D (residues 118 to 480 of human protein) expressed in insect cells and activated by PDK1; and bacterially-expressed GST-AMPK T172D (3 to 308 of rat). Native AMPK was purified from rat liver by Kevin Green in Grahame Hardie's laboratory, University of Dundee. PKB was used at 1 Unit/ml and AMPK at 10 Unit/ml, where 1 Unit is nmole phosphate per min at 30^{o}C incorporated into the substrate peptides Crosstide (GRPRTSSFAEG) for PKB and AMARA peptide (AMARAASAAALARRR) for AMPK. Reactions were carried at 30°C for 30 min when a single kinase was used. Sequential phosphorylation with two kinases was carried out by starting the reaction with the first kinase for 15 min followed by the second kinase for a further 30 min.

Molecular biology

TBC1D1 cDNA was generated by RT-PCR amplification from RNA extracted from HeLa cells, and cloning into the vector pCMV5.HA-1. Bacterial expression plasmids for GST-TBC1D1-full-length and GST-TBC1D1-C-terminal (encoding residues 640 to 1168) were generated by cloning into the vector pGEX6P-1 using standard procedures. Site-directed mutations were introduced into the TBC1D1 coding sequences following the Quickchange protocol (Stratagene) using the KOD HotStart DNA polymerase (Novagene). Sequences of all DNA constructs were checked by the service managed by Nick Helps, University of Dundee (www.dnaseq.co.uk).

Cell culture, stimulations, cross-linking, lysis and immunoprecipitations

Human HEK293 cells cultured on 10-cm diameter dishes in medium containing 10% (v/v) foetal bovine serum were used 30 h after transfection with the indicated plasmids. Rat L6 myoblasts were maintained in medium containing 10% (v/v) foetal bovine serum and differentiated into myotubes in medium containing 2% (v/v) horse serum for 4 days. Cells were serum-starved for 4 h (unstimulated), then stimulated as indicated with IGF1 at 50 ng/ml for 15 min, insulin at 100 nM for 30 min, serum at 10% (v/v) for 15 min, calyculin A at 100 nM for ~5 min, AICAR at 2 mM for 1 h, phenformin at 2 mM for 1 h, A-769662 at 50 µM for 1h, EGF at 50 ng/ml for 15 min, PMA at 100 ng/ml for 30 min and A23187 at 10 µM for 1 h. Where indicated, cells were incubated with LY294002 (100 µM for 1 h), wortmannin (100 nM for 1h), Go6983 (1 µM for 30 min), BI-D1870 (10 µM for 30 min) and AMPK inhibitor Compound C (20 µM for 1 h) prior to stimulation with IGF1 and other stimuli. After stimulation, cells were lysed in 0.3 ml ice-cold lysis buffer as in [16].

TBC1D1/14-3-3 interactions were stabilised during cell lysis and immunoprecipitation by using a reversible chemical crosslinker: Cells were rinsed with cold PBS, lysed in 0.3 ml lysis buffer containing dithiobis[succinimidyl propionate] (DSP, 2.5 mg/ml from 250 mg/ml in DMSO) for 30 min on ice, and unreacted cross-linker was quenched with 75 μl of 1 M Tris-HCl pH 7.4 with a further 30 min incubation [10,17]. For immunoprecipitations with anti-HA and anti-TBC1D1, 3 μg antibody/mg lysate was mixed at 4°C for 2 h, then protein G-Sepharose (30 μl of a 50% suspension in lysis buffer) added and mixed for a further hour. The suspension was centrifuged at 12,000 g for 30 sec between washes. Immunoprecipitates were extracted into

SDS-sample buffer lacking reducing agent, and centrifuged to clarify before adding reducing agent (Invitrogen) to the supernatant.

14-3-3 overlays and Western blots

Membranes were incubated in 50 mM Tris-HCl, pH 7.5, 0.15 M NaCl and 0.2% (v/v) Tween 20 containing 5% (w/v) dried milk powder (Marvel) and were immunoblotted at 4°C for 16 h using the indicated antibodies at 1 μg/ml. Detection was performed using horseradish-peroxidase-conjugated secondary antibodies (Promega) and ECL® (enhanced chemiluminescence reagent; Amersham Biosciences) for all Western blots of endogenous proteins and DIG-14-3-3 overlays (which use DIG-labelled 14-3-3 in place of primary antibody [16]. Western blots of HA-TBC1D1 used Infrared dye-labelled secondary antibodies that were detected using the Odyssey Infrared Imaging System (LI-COR, Inc.).

Identification of phosphorylated residues in HA-TBC1D1 extracted from cells growing in medium containing serum

HA-TBC1D1 was immunoprecipitated from lysates of cells growing in medium containing serum. After SDS-PAGE, the colloidal Coomasie-stained bands were digested with trypsin and analysed by LC-MS on a 4000 Q-TRAP system using precursor ion scanning [18]. If the site of phosphorylation could not be assigned from the msms spectra acquired on this mass spectrometer, a second aliquot of the tryptic digest was analysed by LC-MS on a Thermo-Electron LTQ-orbitrap mass spectrometer coupled to a Dionex 3000 nano liquid chromatography system. Precise masses for the phosphopeptides detected by the precursor ion scanning on the 4000 Q-TRAP were entered into an inclusion list and these ion masses were preferentially selected for msms with multistage activation. The resultant data files were searched against the TBC1D1 sequence, using Mascot run on an in house server, with a 10ppm mass accuracy for precursor ions and phosphorylation of serine/threonine or tyrosine as variable modifications. The individual msms spectra for the phosphopeptide ions were inspected using Xcalibur 2.2 software to assign the site(s) of phosphorylation.

Reproducibility

Except for mass spectrometry experiments, results shown are representative of at least two similar experiments.

RESULTS

Phylogenetic analysis of TBC1D1 and AS160 and identification of phosphorylated sites on TBC1D1

The phylogeny of AS160 and TBC1D1 sequences from animal species suggests that TBC1D1 is the most ancient gene, whereas AS160 emerged with the vertebrates with subsequent sequence divergence generating the distinct TBC1D1 and AS160 that exist today (Fig 1A).

HA-TBC1D1 was extracted from transfected HEK293 cells that were cultured in medium containing serum. Precursor ion scanning of tryptic digests of the extracted protein revealed the presence of eight phosphopeptides, which were then identified by MS/MS as seven singly phosphorylated peptides and one triply phosphorylated peptide (Supplementary Table 1). Six phosphorylated residues could be assigned with confidence, namely Ser237, Ser263, Ser507, Ser565, Ser566 and Thr596, whereas less clear data indicate that Ser585 might also be phosphorylated under these conditions (Supplementary Table 1 and Figs 1B and 1C).

Some of the phosphorylated sites in TBC1D1 are conserved in the amino acid sequence of AS160: Thr596 on TBC1D1 looks similar to pThr642-AS160 (both potential PKB sites), and Ser507 on TBC1D1 looks similar to pSer570 on AS160 (Figs 1B and 1C). There is sufficient divergence however, that matches for the other phosphorylated sites could not have been inferred simply by comparing the aligned sequences.

Identification of pSer237 and pThr596 as 14-3-3-binding sites on TBC1D1

HA-TBC1D1 immunoprecipitated from transfected cells was able to bind directly to 14-3-3 proteins in an overlay (Far-Western) assay (Fig 2A). The binding to 14-3-3s was abolished by dephosphorylation of the TBC1D1 with the protein phosphatase PP2A in vitro, and this was prevented by the PP2A inhibitor microcystin-LR (Fig 2A).

HA-Thr596Ala-TBC1D1 mutant protein extracted from cells growing in serum still bound to 14-3-3s, albeit to a lesser extent than the wild-type protein, indicating that 14-3-3s bind to both phosphoThr596 and a second 14-3-3-binding site on TBC1D1 (Fig 2B). Binding of 14-3-3s to HA-Thr596Ala-TBC1D1 was also abolished by dephosphorylation, showing that the second interaction with 14-3-3s is also phosphorylation-dependent (Fig 2C).

The PAS antibody recognizes proteins that have been phosphorylated within RXRXXpS/T motifs. Both the anti-PAS and 14-3-3 binding signals for wild-type HA-TBC1D1

were increased when the protein was extracted from IGF1-stimulated cells, compared with unstimulated cells (Fig 2D). The Thr596Ala mutation largely abolished binding of the anti-PAS antibody and also blunted the IGF1-induced 14-3-3 binding (Fig 2B, C, D). Previously, we had identified two 14-3-3 binding sites flanking the second PTB domain on AS160 [10], and we hypothesized that this might also be true for TBC1D1. Of the phosphorylation sites identified (Supplementary Table 1), phosphoSer237 conforms to the Mode 1 14-3-3-binding consensus [http://scansite.mit.edu/motifscan_seq.phtml; 19] and was an obvious candidate for the second 14-3-3-binding site on TBC1D1. Consistent with this possibility, the double mutant HA-Ser237Ala/Thr596Ala-TBC1D1 was unable to bind to 14-3-3s (Fig 2D).

PhosphoThr596 mediates 14-3-3-binding in response to IGF1, whereas phosphorylation of Ser237 is required for 14-3-3-binding in response to IGF1/LY294002

The anti-PAS and 14-3-3 overlay signals, and amounts of co-immunoprecipitating endogenous 14-3-3s, were increased when HA-TBC1D1 was extracted from serum-, IGF1- and calyculin A-stimulated HEK293 cells, compared with unstimulated (serum-starved) cells (Fig 2E). In contrast, the binding of 14-3-3s to HA-Thr596Ala-TBC1D1 was not increased by serum and IGF1 (Fig 2E).

The trace anti-PAS signal seen in the lanes containing HA-Thr596Ala-TBC1D1 can be attributed to co-immunoprecipitation of the endogenous AS160, which was detected by Western blotting (Fig 2E). HA-TBC1D1 and GST-AS160 were also found to co-immunoprecipitate from extracts of doubly transfected cells (Supplementary Fig 1), though whether this represents a physiologically significant interaction is not known.

Consistent with phosphorylation of Thr596 being stimulated via PI 3-kinase, the IGF1-induced anti-PAS signal for HA-TBC1D1 was markedly decreased when cells were preincubated with the PI 3-kinase inhibitor LY294002 (Fig 2E). This inhibitor blocked the IGF1-induced phosphorylation of Thr308 of PKB, as expected. In contrast, LY294002 did not inhibit the binding of 14-3-3s to wild-type HA-TBC1D1 as determined in the overlay assay, and by co-precipitation of endogenous 14-3-3s with the extracted HA-TBC1D1 (Fig 2E). Moreover, 14-3-3-binding to HA-Thr596Ala-TBC1D1 was actually enhanced by treatment of cells with LY294002 (Fig 2E). As reported previously [10], we found that LY294002 induces phosphorylation of the activating site on AMPK in HEK293 cells (Fig 2E). Thus, these findings suggested the hypothesis that 14-3-3-binding might be enhanced by LY294002-

activated phosphorylation of Ser237 by AMPK. Phosphorylated Ser237 is in a site that conforms to the consensus for phosphorylation by AMPK [8].

To investigate the phosphorylation of Thr596 and Ser237 in more detail, we raised phospho-specific antibodies against these sites. Both the pThr596-TBC1D1 and pSer237-TBC1D1 antibodies specifically recognised the appropriate phosphopeptide immunogens, but not the corresponding dephosphorylated peptides (Supplementary Fig 2A, B) nor the phosphopeptide corresponding to the other site (data not shown). The pThr596-TBC1D1 antibody showed some cross-reactivity with AS160 extracted from IGF1-stimulated cells, presumably because pThr642 on AS160 is within a similar sequence (Supplementary Fig 2E). It is not a problem to distinguish TBC1D1 and AS160 however, because AS160 runs above TBC1D1 on SDS-PAGE and can be detected with the anti-AS160 antibodies, which do not react with TBC1D1 (Fig 2E; Supplementary Fig 2D). When tested on HA-TBC1D1 extracted from serum-grown cells, the signal for each phosphospecific antibody was abolished when the appropriate residue was mutated to Ala (Supplementary Fig 2C).

Use of the pThr596 antibody confirmed that phosphorylation of Thr596 in TBC1D1 was induced by serum, IGF1 and calyculin A, and abolished by LY294002 (Fig 2E). In contrast, the phosphoSer237-TBC1D1 antibody data showed that phosphorylation of Ser237 is increased in response to LY294002 (Fig 2E), consistent with possible phosphorylation by AMPK and with phosphoSer237 being responsible for LY294002-induced 14-3-3 binding (Fig 2E).

Because of the peculiarity of LY294002 in activating AMPK in HEK293 cells, we compared its effects with those of a second PI 3-kinase inhibitor, wortmannin. In cells stimulated with IGF1 without inhibitors, the binding of 14-3-3s to HA-TBC1D1 mirrored the phosphorylation of Thr596 and 14-3-3 binding was lost in the Thr596Ala mutant (Fig 3, left hand side). Wortmannin markedly reduced both phosphorylation of Thr596 and binding of 14-3-3s to TBC1D1 (Fig 3, right hand side). No obvious activation of AMPK was observed with wortmannin (later results). In contrast, the wild-type protein extracted from cells treated with LY294002 displayed strong 14-3-3-binding despite inhibition of Thr596 phosphorylation (Fig 3 middle lanes). Moreover, the binding of 14-3-3s to HA-TBC1D1 from LY294002-treated cells was unaffected by the Thr596Ala mutation, but lost in the Ser237Ala mutant (Fig 3). Thus, phosphoThr596 is the highest affinity 14-3-3-binding site generated in response to IGF1, and phosphorylation of Thr596 is blocked by both PI 3-kinase inhibitors (Fig 2E and 3). In

addition, LY294002 induces 14-3-3-binding by promoting phosphorylation of Ser237 (Fig 2E and 3), and AMPK, which is activated by LY294002 in these cells (Fig 2E), became a candidate Ser237-TBC1D1 kinase.

Regulation of Ser237 and Thr596 phosphorylation and 14-3-3 binding of TBC1D1 in response to different stimuli in HEK293 cells

Using a wider variety of cellular stimuli, the binding of 14-3-3s to HA-TBC1D1 was enhanced when cells were stimulated with serum, the growth factors IGF1 and EGF, AMPK activators AICAR and phenformin, the phorbol ester PMA, adenylate cyclase activator forskolin, and calcium ionophore A23187 (Fig 4). The strongest 14-3-3-binding signals were seen with HA-TBC1D1 from cells stimulated by IGF1 and phenformin. The 14-3-3 overlay signal for extracted HA-TBC1D1 mirrored the results for co-immunoprecipitation of endogenous 14-3-3s (Fig 4).

The various stimuli induced distinct patterns of phosphorylation of Ser237 and Thr596 of HA-TBC1D1. The phosphorylation of Thr596 was increased in response to serum, IGF1, EGF, PMA and forskolin. In contrast, phenformin and A23187 promoted a stronger phosphorylation of Ser237, compared with Thr596 (Fig 4 and data not shown). These findings are consistent with the possibility that AMPK phosphorylates Ser237. These data also indicate that binding of 14-3-3s to HA-TBC1D1 may depend on either pSer237 and/or pThr596 to different extents in cells stimulated in different ways.

Mutation of Ser237 and Thr596 has differential effects on 14-3-3 binding of TBC1D1 in response to different stimuli in HEK293 cells

HA-TBC1D1 with mutated Ser237 and/or Thr596 was tested for its binding to 14-3-3s after extraction from cells exposed to the various stimuli (Fig 5). A general observation is that the double mutant HA-Ser237Ala/Thr596Ala-TBC1D1 did not co-precipitate with endogenous 14-3-3s in response to any of the stimuli tested (Fig 5A to G). Similarly, the HA-Ser237Ala/Thr596Ala-TBC1D1 mutant extracted from the variously-stimulated cells was unable to bind to 14-3-3s in the overlay assay (data not shown).

The analysis of the mutants indicated that basal binding of 14-3-3s to HA-TBC1D1 in the unstimulated (serum-starved) cells is primarily attributable to basal phosphorylation of Ser237, with a trace of Thr596 phosphorylation (Figs 4 and 5A). Similar to the results seen with IGF1 (Fig 3), the binding of 14-3-3s to HA-TBC1D1 extracted from cells stimulated with

serum, EGF and PMA was most severely abrogated by mutation of Thr596, whereas the Ser237Ala mutation had a lesser effect (Figs 5B to D). These data are consistent with Thr596 phosphorylation being induced by EGF and PMA (Fig 4). For HA-TBC1D1 from forskolin-treated cells, the binding of 14-3-3s was partially reduced by mutation of either Ser237 or Thr596 (Figs 5E). In contrast, the interaction between 14-3-3s and HA-TBC1D1 from phenformin-stimulated cells was most strongly inhibited by mutation of Ser237 (Fig 5F). This result is similar to that seen with IGF1/LY294002 (Figs 2E and 3), and is consistent with AMPK being the Ser237 kinase. Binding of 14-3-3s to TBC1D1 extracted from cells treated with calcium ionophore A23187 was also dependent on Ser237 (Fig 5G and data not shown).

Effect of inhibitors on TBC1D1 phosphorylation and 14-3-3 binding TBC1D1 in response to different stimuli in HEK293 cells

Consistent with phosphorylation by AMPK, the AMPK inhibitor Compound C [20] partially inhibited the phosphorylation of Ser237 and 14-3-3 binding in response to phenformin (Fig 6A, last two lanes), and Compound C also partially inhibited the lesser responses to metformin and AICAR (Fig 6A). Wortmannin inhibited both the IGF1- and EGF-induced phosphorylation of Thr596 (Fig 6B). In contrast, the RSK-specific inhibitor BI-D1870 [21] and non-specific PKC inhibitor Go6983 prevented the PMA-induced phosphorylation of Thr596, consistent with the PKC/Erk/RSK pathway mediating the regulation of this site in response to PMA. In cells stimulated with EGF and PMA, BI-D1870 caused a slight increase in phosphorylation of Ser237 of TBC1D1 concomitant with a stimulation of AMPK and ACC phosphorylation (Fig 6B and data not shown).

In vitro phosphorylation of GST-TBC1D1 by PKB and AMPK

Purified bacterially-expressed GST-TBC1D1 comprised full-length protein and truncated proteins that were missing variously-sized portions from the C-terminus (Fig 7A).

Native and recombinant AMPK phosphorylated several residues on GST-TBC1D1 (Ser237, Ser487 or Thr489, Ser503 or Thr505, Ser558 or Ser559, Thr596), as determined using phosphospecific pSer237-TBC1D1 and pThr596-TBC1D1 antibodies (Fig 7) and mass spectral analysis of tryptic digests (not shown). The AMPK-phosphorylated forms of GST-TBC1D1 that were >50 kDa could bind strongly to 14-3-3s, including fragments that were too small to contain phosphorylated Thr596 (Fig 7D). We also noticed that AMPK induced a slight

upwards band-shift in the GST-TBC1D1 fragment that runs at ~110 kDa (most obvious in Fig 7C).

In contrast, PKB phosphorylated Ser235 (mass spectral data, not shown) and Thr596 (Fig 7C), but did not phosphorylate Ser237 (Fig 7B), and did not induce the GST-TBC1D1 to bind to 14-3-3s (Fig 7D). Moreover, prior phosphorylation with PKB inhibited subsequent AMPK-induced phosphorylation of Ser237 (Fig 7B) and binding of GST-TBC1D1 to 14-3-3s (Fig 7D), and PKB also prevented the AMPK-induced upwards band-shift in the ~110 kDa protein (Fig 7C). In contrast, GST-TBC1D1 that was phosphorylated first by AMPK and then by PKB could bind to 14-3-3s (Fig 7D), and displayed the upwards band-shift of the ~110 kDa fragment (Fig 7C).

The in vitro phosphorylations were repeated with GST-TBC1D1-Ser235Ala mutant protein. In contrast to the wild-type protein, prior phosphorylation of the Ser235Ala-TBC1D1 mutant with PKB did not prevent subsequent AMPK-mediated Ser237 phosphorylation and 14-3-3 binding (Supplementary Fig 3). These data indicate that in vitro phosphorylation of Ser235 by PKB was responsible for preventing the AMPK-induced phosphorylation of Ser237 and/or AMPK-induced binding of wild-type GST-TBC1D1 to 14-3-3s.

Complementary phosphorylation and 14-3-3-binding of endogenous TBC1D1 and AS160 in response to insulin and AMPK activators in rat L6 myotubes

Using an antibody raised against the C-terminal 529 amino acids of the protein, sufficient endogenous TBC1D1 for analysis could be immunoprecipitated from rat L6 myotubes (Fig 8A), but not from HEK293 cells or adipocytes. From a Coomassie-stained SDS-gel of the immunoprecipitate, four protein bands of ~ 140-150 kDa were identified as forms of TBC1D1 (not shown). These forms of TBC1D1 correspond to the four bands seen in the top four panels of Fig 8A. In addition, a protein of 110 kDa was identified as TBC1D2, another GAP protein that is likely to cross-react with the anti-TBC1D1 antibody (not shown). When the myotubes were stimulated with insulin, the activating Thr308 of PKB and Thr596 of TBC1D1 were phosphorylated (Fig 8A), and both phosphorylations were inhibited by wortmannin. However, insulin did not promote any obvious binding of 14-3-3s to the TBC1D1 (Fig 8A). In contrast, phenformin promoted a robust activation of AMPK, phosphorylation of Ser237 of TBC1D1, 14-3-3-overlay signal and co-precipitation of 14-3-3s (Fig 8A). A-769662, a recently described small molecule AMPK activator [22,23], also promoted a strong phosphorylation of

Ser237 of the endogenous TBC1D1, together with strong binding of 14-3-3s and co-precipitation of 14-3-3s with the isolated TBC1D1 (Fig 8A).

Consistent with previous observations [10] and in contrast to TBC1D1, the endogenous AS160 was phosphorylated on both its 14-3-3 binding sites and bound to 14-3-3s when L6 myotubes were stimulated with insulin, but not when AMPK was activated by A-769662 in these cells (Fig 8B).

Co-localisation of endogenous TBC1D1 and GluT4 in rat L6 myotubes

In immunocytochemistry experiments with unstimulated rat L6 myotubes, the anti-TBC1D1 and anti-GluT4 glucose transporter antibodies both gave signals that were associated with perinuclear structures (Fig 8C). With the caveat that the anti-TBC1D1 antibody also recognises TBC1D2, these findings are consistent with TBC1D1 and GluT4 being located near to each other. When cells were stimulated with either insulin or A-769662, GluT4 staining was seen at the cell surface in a proportion (~10 to 15%) of cells. Presumably, the other cells were not sufficiently differentiated to be fully responsive to these stimuli. It was notable however, that cells with cell surface staining for anti-GluT4 also displayed more prominent cell surface localisation for anti-TBC1D1, suggesting that in these cells TBC1D1 accompanies GluT4 during its well-characterised translocation to the plasma membrane (Fig 8C).

DISCUSSION

Phylogenetic analysis suggests that AS160 evolved with the vertebrates, whereas TBC1D1 is more ancient, being found in all animals examined (Fig 1A). We speculate that AS160 arose to provide more versatile upstream regulation of the Rabs that may be common substrates of these RabGAPs [4]: The GAP domains are conserved, whereas AS160 and TBC1D1 sequences diverge most in the N-terminal tail and within the two distinct clusters of phosphorylated sites that are located either side of the second PTB domain in both AS160 and TBC1D1 (Fig 1B, C). Notable exceptions are the identical short sequences surrounding the phosphorylatable Thr596 in TBC1D1, which corresponds to Thr642 in AS160; and Ser507 in TBC1D1, which is equivalent to Ser570 in AS160 (Fig 1B). Thr568, which can be phosphorylated by SGK in AS160 [10], also finds a match in Ser505 of TBC1D1, though whether Ser505 can be phosphorylated is unknown.

14-3-3s pick out specific binding sites within each phosphorylated cluster, and the simplest hypothesis is that a 14-3-3 dimer straddles the PTB2 domain by binding to phosphoSer237 and phosphoThr596 in TBC1D1, and phosphoSer341 and phosphoThr642 in AS160 (Fig 1B). There are however, clear differences between TBC1D1 and AS160 with respect to the signalling pathways that target these sites and the relative importance of each site for 14-3-3-binding.

For AS160, phosphoThr642 is the high affinity site for binding to 14-3-3s in response to IGF1, EGF and PMA in HEK293 cells [10,11] whereas phosphoSer341 is a lower affinity 14-3-3-binding site [10]. Consistent with previous findings [10], insulin stimulated phosphorylation of Ser341 and Thr642 and binding of 14-3-3s to AS160 in L6 cells, but AMPK activators have little effect (Fig 8B).

In contrast, it appears that either pSer237 or pThr596 of TBC1D1 can take the lead in mediating 14-3-3-binding in response to different stimuli: 14-3-3 binding to TBC1D1 is dominated by phosphorylation of Ser237 in HEK293 cells containing active AMPK, whereas Thr596 is more important for 14-3-3 binding in response to IGF1, EGF and PMA (Figs 3,4,5). In contrast to AS160, insulin stimulated the phosphorylation of Thr596 of TBC1D1, but did not induce phosphorylation of Ser237 or binding to 14-3-3s in L6 cells. Thus, there is a complementarity in that insulin promotes binding of 14-3-3s to AS160, whereas AMPK activators promote binding of 14-3-3s to TBC1D1 in L6 cells.

It is not clear why IGF1 can promote 14-3-3 binding to TBC1D1 via phosphoThr596 in HEK293 cells, and yet insulin stimulated the phosphorylation of Thr596 of TBC1D1, but not its 14-3-3 binding, in L6 cells. One possibility is that the phosphorylation status of other residues in the clusters have positive or negative effects on the phosphorylation and/or binding to 14-3-3s. We found for example, that 14-3-3s cannot bind to TBC1D1 that has been phosphorylated in vitro by PKB, despite this kinase promoting robust phosphorylation of Thr596 (Fig 7). Moreover, both the phosphoSer237 and 14-3-3-binding signals of AMPK-phosphorylated TBC1D1 were markedly inhibited by prior phosphorylation by PKB. Our findings suggest that in vitro phosphorylation of Ser235 by PKB prevents subsequent phosphorylation of Ser237 by AMPK. We do not yet know whether Ser235 is a physiological phosphorylation site, nor do we understand why phosphorylation of Thr596 by PKB does not allow binding of 14-3-3s, even in the form of TBC1D1 where Ser235 is mutated to Ala (Supplementary Fig 3). These data

indicate that there is much to learn about the hierarchies and regulatory interactions amongst the sites of multisite phosphorylation of TBC1D1.

Another finding is that combinations of IGF1/LY294002, EGF/BI-D1870 and PMA/BI-D1870 promote phosphorylation of the activating Thr172 of AMPK and hence phosphorylation of the AMPK substrate acetyl-CoA carboxylase (Fig 4 and 6). To our knowledge, these effects have not been reported previously, though inhibitors of the MAP kinase pathway [24] and human EGF receptor 2 in combination with EGF receptor tyrosine kinase inhibitors [25] have been reported to activated the AMPK. We have made similar observations when studying another protein that is targeted for multisite phosphorylation, and the mechanisms of AMPK activation by these inhibitors are under investigation in HEK293 and other cell types (Jane Murphy and Carol MacKintosh, unpublished). Another AMPK-related puzzle is why phenformin does not promote phosphorylation of Thr596 of TBC1D1 (Fig 4 and 8A), whereas AMPK can phosphorylate this residue in vitro (Fig 7 and Supplementary Fig 2).

Finding that TBC1D1 and GluT4 co-localise with each other in unstimulated, and insulin- and A-769662-responsive rat L6 myotubes (Fig 8C) is consistent with a role for this RabGAP in GluT4 trafficking. The relative roles of TBC1D1 and AS160 are not yet known, but finding that they are subject to complementary regulation suggests that these two proteins may cooperate to mediate responsiveness of glucose uptake to insulin, the anti-diabetic drug metformin, and exercise. The effects of forskolin on AS160 [10] and TBC1D1 (Fig 4) suggest that it might also be worth revisiting the question of whether adrenaline acting via PKA can influence glucose uptake into skeletal muscle [26]. Whether the TBC1D1 phosphorylation in response to the calcium ionophore A23187 is mediated via AMPK or by direct phosphorylation by a calcium-activated protein kinase is not yet known.

AS160 and TBC1D1 have a wider cellular and tissue distribution than GLUT4 however, which means that GLUT4 storage vesicles are unlikely to be the only vesicles whose trafficking is regulated by these RabGAPs. For example, PKB is implicated in trafficking of CD89 to class II-containing vesicles and class II Ag presentation [27], and it is possible that AS160 and TBC1D1 may be PKB targets in this and/or other processes. The antibodies generated here should be useful for defining the relative roles and regulation of TBC1D1 and AS160 in different cell and tissues.

Acknowledgements

This work was supported by Diabetes UK, the U.K. Medical Research Council, the U.K. Biotechnology and Biological Sciences Research Council (grant BB/C511613/1 for mass spectrometry), and the companies who support the Division of Signal Transduction Therapy (DSTT) at the University of Dundee, namely AstraZeneca, Boehringer Ingelheim, GlaxoSmithKline, Merck and Co, Merck KGaA, and Pfizer. We thank Natalia Shpiro, MRC Protein Phosphorylation Unit, University of Dundee for synthesis of A-769662. Thanks to Claire Balfour for tissue culture support, the DSTT antibody and protein production team coordinated by James Hastie for purification of antibodies and bacterially-expressed GST-fusion protein, and Rachel Naismith for secretarial assistance.

RFERENCES

1. Grosshans, B.L., Ortiz, D. and Novick, P. (2006) Rabs and their effectors: achieving specificity in membrane traffic. Proc. Natl. Acad. Sci. U.S.A. **103**, 11821-11827
2. Takai, Y., Sasaki, T. and Matozaki, T. (2001) Small GTP-binding proteins. Physiol. Rev. **81**, 153-208
3. Sano, H., Kane, S., Sano, E., Miinea, C.P., Asara, J.M., Lane, W.S., Garner, C.W. and Lienhard, G.E. (2003) Insulin-stimulated phosphorylation of a Rab GTPase-activating protein regulates GLUT4 translocation. J. Biol. Chem. **278**, 14599-14602
4. Roach, W.G., Chavez, J.A., Miinea, C.P. and Lienhard, G.E. (2007) Substrate specificity and effect on GLUT4 translocation of the Rab GTPase activating protein Tbc1d1. Biochem. J. **403**, 353-358.
5. Dugani, C.B. and Klip, A. (2005) Glucose transporter 4: cycling, compartments and controversies. EMBO Rep. **6**, 1137-1142
6. Hou, J.C. and Pessin, J.E. (2007) Ins (endocytosis) and outs (exocytosis) of GLUT4 trafficking. Curr. Opin. Cell Biol. **19**, 1-8
7. Matsumoto, Y., Imai, Y., Lu Yoshida N, Sugita Y, Tanaka T, Tsujimoto G, Saito H, Oshida T. (2004) Upregulation of the transcript level of GTPase activating protein KIAA0603 in T cells from patients with atopic dermatitis. FEBS Lett. **572**, 135-140

8. Stone, S., Abkevich, V., Russell, D.L., Riley, R., Timms, K., Tran, T., Trem, D., Frank, D., Jammulapati, S., Neff, C.D., Iliev, D., Gress, R., He, G., Frech, G.C., Adams, T.D., Skolnick, M.H., Lanchbury, J.S., Gutin, A., Hunt, S.C. and Shattuck, D. (2006) TBC1D1 is a candidate for a severe obesity gene and evidence for a gene/gene interaction in obesity predisposition. Hum. Mol. Genet. **15**, 2709-2720

9. Kane, S., Sano, H., Liu, S.C., Asara, J.M., Lane, W.S., Garner, C.C. and Lienhard, G.E. (2002) A method to identify serine kinase substrates. Akt phosphorylates a novel adipocyte protein with a Rab GTPase-activating protein (GAP) domain. J. Biol. Chem. **277**, 22115-22118

10. Geraghty, K.M., Chen, S., Harthill, J.E., Ibrahim, A.F., Toth, R., Morrice, N.A., Vandermoere, F., Moorhead, G.B., Hardie, D.G. and MacKintosh, C. (2007) Multisite phosphorylation and 14-3-3 binding of AS160 in response to IGF1, insulin, and AICAR. Biochem. J. **407**, 231-241

11. Ramm, G., Larance, M., Guilhaus, M. and James, D.E. (2006) A role for 14-3-3 in insulin-stimulated GLUT4 translocation through its interaction with the RabGAP AS160. J. Biol. Chem. **281**, 29174-29180

12. Kramer, H.F., Witczak, C.A., Taylor, E.B., Fujii, N., Hirshman, M.F. and Goodyear, L.J. (2006) AS160 regulates insulin- and contraction-stimulated glucose uptake in mouse skeletal muscle. J. Biol. Chem. **281**, 31478-31485

13. Stone, S., Abkevich, V., Hunt, S.C., Gutin, A., Russell, D.L., Neff, C.D., Riley, R., Frech, G.C., Hensel, C.H., Jammulapati, S., Potter, J., Sexton, D., Tran, T., Gibbs, D., Iliev, D., Gress, R., Bloomquist, B., Amatruda, J., Rae, P.M., Adams, T.D., Skolnick, M.H. and Shattuck, D. (2002) A major predisposition locus for severe obesity, at 4p15-p14. Am. J. Hum. Genet. **70**, 1459-1468

14. Arya, R., Duggirala, R., Jenkinson, C.P., Almasy, L., Blangero, J., O'Connell, P. and Stern, M.P. (2004) Evidence of a novel quantitative-trait locus for obesity on chromosome 4p in Mexican Americans. Am. J. Hum. Genet. **74**, 272-282 (Erratum in Am. J. Hum. Genet. (2004) **74**, 1080)

15. Jin, J., Smith, F.D., Stark, C., Wells, C.D., Fawcett, J.P., Kulkarni, S., Metalnikov, P.,

O'Donnell, P., Taylor, P., Taylor, L., Zougman, A., Woodgett, J.R., Langeberg, L.K., Scott, J.D. and Pawson, T. (2004) Proteomic, functional, and domain-based analysis of in vivo 14-3-3 binding proteins involved in cytoskeletal regulation and cellular organization. Curr. Biol. **14**, 1436-1450

16. Pozuelo Rubio, M., Geraghty, K.M., Wong, B.H., Wood, N.T., Campbell, D.G., Morrice, N. and MacKintosh, C. (2004) 14-3-3-affinity purification of over 200 human phosphoproteins reveals new links to regulation of cellular metabolism, proliferation and trafficking. Biochem. J. **379**, 395-408

17. Kim, D.H., Sarbassov, D.D., Ali, S.M., King, J.E., Latek, R.R., Erdjument-Bromage, H., Tempst, P. and Sabatini, D.M. (2002) mTOR interacts with raptor to form a nutrient-sensitive complex that signals to the cell growth machinery. Cell **110**, 163-175

18. Williamson, B. L., Marchese, J. and Morrice, N. A. (2006) Automated identification and quantification of protein phosphorylation sites by LC/MS on a hybrid triple quadrupole linear ion trap mass spectrometer. Mol. Cell. Proteomics **5**, 337-346

19. Obenauer, J.C., Cantley, L.C. and Yaffe, M.B. (2003) Scansite 2.0: Proteome-wide prediction of cell signaling interactions using short sequence motifs. Nucleic Acids Res. **31**, 3635-3641

20. Lee, M., Hwang, J.T., Lee, H.J., Jung, S.N., Kang, I., Chi, S.G., Kim, S.S. and Ha, J. (2003) AMP-activated protein kinase activity is critical for hypoxia-inducible factor-1 transcriptional activity and its target gene expression under hypoxic conditions in DU145 cells. J. Biol. Chem. **278**, 39653-39661

21. Sapkota, G.P., Cummings, L., Newell, F.S., Armstrong, C., Bain, J., Frodin, M., Grauert, M., Hoffmann, M., Schnapp, G., Steegmaier, M., Cohen, P. and Alessi, D.R. (2007) BI-D1870 is a specific inhibitor of the p90 RSK (ribosomal S6 kinase) isoforms in vitro and in vivo. Biochem. J. **401**, 29-38

22. Cool, B., Zinker, B., Chiou, W., Kifle, L., Cao, N., Perham, M., Dickinson, R., Adler, A., Gagne, G., Iyengar, R., Zhao, G., Marsh, K., Kym, P., Jung, P., Camp, H.S. and Frevert, E. (2006) Identification and characterization of a small molecule AMPK activator that treats key components of type 2 diabetes and the metabolic syndrome. Cell

Metab. **3**, 403-416

23. Göransson, O., McBride, A., Hawley, S.A., Ross, F.A., Shpiro, N., Foretz, M., Viollet, B., Hardie, D.G. and Sakamoto, K. Mechanism of action of A-769662, a valuable tool for activation of AMP-activated protein kinase. (submitted)

24. Dokladda, K., Green, K.A., Pan, D.A. and Hardie, D.G. (2005) PD98059 and U0126 activate AMP-activated protein kinase by increasing the cellular AMP:ATP ratio and not via inhibition of the MAP kinase pathway. FEBS Lett. **579**, 236-240 (Erratum in FEBS Lett. (2005) **579**, 2019)

25. Spector, N.L., Yarden, Y., Smith, B., Lyass, L., Trusk, P., Pry, K., Hill, J.E., Xia, W., Seger, R. and Bacus, S.S. (2007) Activation of AMP-activated protein kinase by human EGF receptor 2/EGF receptor tyrosine kinase inhibitor protects cardiac cells. Proc. Natl. Acad. Sci. U.S.A. **104**, 10607-10612

26. Bonen, A., Megeney, L.A., McCarthy, S.C., McDermott, J.C. and Tan, M.H. (1992) Epinephrine administration stimulates GLUT4 translocation but reduces glucose transport in muscle. Biochem. Biophys. Res. Commun. **187**, 685-691

27. Lang, G.A. and Lang, M.L. (2006) Protein kinase Balpha is required for vesicle trafficking and class II presentation of IgA Fc receptor (CD89)-targeted antigen. J. Immunol. **176**, 3987-3994

28. Thompson, J.D., Gibson, T.J., Plewniak, F., Jeanmougin, F. and Higgins, D.G. (1997) The CLUSTAL_X windows interface: flexible strategies for multiple sequence alignment aided by quality analysis tools. Nucleic Acids Res. **25**, 4876-4882

29. Kane, S. and Lienhard, G.E. (2005) Calmodulin binds to the Rab GTPase activating protein required for insulin-stimulated GLUT4 translocation. Biochem. Biophys. Res. Commun. **335**, 175-180

Figure legends

Figure 1 Sequence alignment and phylogenetic analysis of AS160 (TBC1D4) and TBC1D1

A. Sequences were aligned using the ClustalX programme [28], with gaps included. A neighbour-joining tree was constructed with *Saccharomyces cerevisiae* Gyp5Pp as the root, and viewed with NJplot. The scale bar indicates the number of substitutions per position for the branch length indicated. The protein sequences were derived from the following Genbank and Ensembl sources: AaTBC1D1 (EAT41590); AgTBC1D1 (EAA13644); AmTBC1D1 (XP_392862); BtTBC1D1 (XP_611974); CfTBC1D1 (XP_536262); Dp TBC1D1 (EAL28187); DrTBC1D1 (ENSDARP00000083727); GaTBC1D1 (ENSGACP00000021282); GgTBC1D1 (XP_423827); HsTBC1D1 (NP_055988); MmTBC1D1 (XP_001087581); Mouse TBC1D1 (BAE32696); OlTBC1D1 (ENSORLP00000006807); DmTBC1D1 (CAA76939); PtTBC1D1 (XP_001137680); RnTBC1D1 (XP_341216); SpTBC1D1 (XP_789662); TrTBC1D1 (NEWSINFRUP00000173789); XtTBC1D1 (CAJ81274); *S. cerevisiae* GYP5p (NP_015075); BtAS160/TBC1D4 (XP_879978); CfAS160/TBC1D4 (XP_542613); DrAS160/TBC1D4 (XP_687662); GaAS160/TBC1D4 (ENSGACP00000002437); GgAS160/TBC1D4 (ENSGALP00000027310); HsAS160 (NP_055647); MmAS160/TBC1D4 (ENSMMUP00000027914); Mouse AS160/TBC1D4 (XP_924145); OlAS160/TBC1D4 (ENSORLP00000014171); PpAS160/TBC1D4 (CAH90731); PtAS160/TBC1D4 (ENSPTRP00000010082); RnAS160/TBC1D4 (XP_001074183); TnAS160/TBC1D4 (CAG07307); TrTBC1D4 (NEWSINFRUP00000160242); XlAS160/TBC1D4 (AAH73710); XtAS160/TBC1D4 (ENSXETP00000010226). Abbreviations are: Aa, *Aedes aegypti*; Ag, *Anopheles gambiae* str. PEST; Am, *Apis mellifera*; Bt, *Bos taurus*; Cf, *Canis familiaris*; Dm, *Drosophila melanogaster*; Dp, *Drosophila pseudoobscura*; Dr, *Danio rerio*; Ga, *Gasterosteus aculeatus*; Gg, *Gallus gallus*; Hs, *Homo sapiens*; Mm, *Macaca malatta*; Ol, *Oryzias latipes*; Pp, *Pongo pygmaeus*; Pt, *Pan troglodytes*; Rn, *Rattus norvegicus*; Sc, *Saccharomyces cerevisiae*; Sp, *Strongylocantrotus purpuratus*; Tr, *Takifugu rubripes*; Xl, *Xenopus laevis*; Xt, *Xenopus tropicalis*.

B. Outline structures of AS160 and TBC1D1 indicating in grey shading the PTB1, PTB2, a calmodulin binding motif (CBD) in AS160 [29] and the corresponding motif in TBC1D1, and TBC1D1 (RabGAP) domains. The amino acid residue numbers at the borders of these domains

are indicated. Also indicated are the R125W mutation site in TBC1D1 [8], and a site on AS160 where alternative exon usage generates a longer splice variant (this shorter form is termed AS160A and the longer form AS160B; [10]). The positions of phosphorylated sites on AS160 [3,10] and TBC1D1 ([4] and this study) are shown, with the two 14-3-3-binding sites on each protein highlighted by boxes [10,11, this study]. Ser235 was identified as an in vitro phosphorylated site (see later results) and whether it is phosphorylated physiologically is not known.

C. Sequences of human AS160 and TBC1D1 in the regions of the first and second clusters of phosphorylated residues. This alignment is extracted from the ClustalX analysis of all the sequences used for Fig 1A, and differs from the BLAST alignment that was obtained by aligning only the sequences of the two human proteins (supplementary data in [10]). Phosphorylated residues are in bold and underlined. The numbers of the phosphorylated residues are indicated, with a question mark at Ser585 of TBC1D1 to indicate an uncertain assignment, and boxed residues to show the two 14-3-3 binding sites on each protein.

Figure 2 Phosphorylation-dependent binding of 14-3-3 to HA-TBC1D1 extracted from transfected HEK293 cells

A. HA-TBC1D1 immunoprecipitated with anti-HA from lysates (200 μg) of cells cultured in medium containing serum was incubated with 50 milliunits/ml PP2A, with or without microcystin-LR (MC-LR; 5 μM) and analysed with the anti-PAS antibody and for 14-3-3 binding in the overlay assay.

B. HA-TBC1D1 and HA-Thr596Ala-TBC1D1 immunoprecipitated from lysates of cells cultured in medium containing serum was analysed with the anti-PAS antibody and for 14-3-3 binding in the overlay assay.

C. HA-Thr596Ala-TBC1D1 from cells growing with serum was incubated with 50 milliunits/ml PP2A, with or without microcystin-LR (MC-LR; 5 μM) and analysed for 14-3-3 binding in the overlay assay.

D. HA-TBC1D1, HA-Thr596Ala-TBC1D1 and HA-Ser237Ala/Thr596Ala-TBC1D1 immunoprecipitated from lysates prepared in the presence of DSP from unstimulated (U) and IGF1-stimulated (I) cells was analysed with the anti-PAS antibody and for 14-3-3 binding in the overlay assay. Co-precipitating 14-3-3s were detected by Western blotting with the K19 antibody (Santa Cruz).

E. HA-TBC1D1 and HA-Thr596Ala-TBC1D1 immunoprecipitated from lysates (0.5 mg) prepared in the presence of DSP from cells that were unstimulated, serum-stimulated, IGF1-stimulated, IGF1-stimulated in the presence of LY294002, and treated with calyculin A. Immunoprecipitates were analysed by Western blotting with the anti-HA, anti-PAS, anti-AS160 and anti-14-3-3 (K19) antibodies, and by 14-3-3 overlay assays, as indicated. For the bottom seven panels, lysates (40 μg) were analysed with antibodies to monitor levels of total HA-TBC1D1, AMPK, total PKB and the phosphorylation status these proteins (pSer237-TBC1D1, pThr596-TBC1D1, pThr172-AMPK and pThr308-PKB).

Figure 3 Comparison of the effects of LY294002 and wortmannin on the phosphorylation and 14-3-3 binding of HA-TBC1D1

HA-TBC1D1, the Thr596Ala and Ser237Ala single mutants, and Ser237Ala/Thr596Ala double mutant were immunoprecipitated from lysates of cells that had been stimulated with IGF1 alone, or after preincubation with LY or wortmannin (WM). The extracted proteins were analysed with the phosphospecific pSer237-TBC1D1 and pThr596-TBC1D1 antibodies, and co-precipitating 14-3-3s were identified using the K19 antibody.

Figure 4 Effects of different cellular stimuli on the multisite phosphorylation and 14-3-3 binding of HA-TBC1D1

HA-TBC1D1 from cells exposed to various stimuli (as specified in Materials and Methods) was analysed with phosphospecific antibodies that recognise phosphorylated Ser237 and Thr596. Anti-HA control blots are shown for each phospho-specific antibody blot. The 14-3-3 binding capacity of the HA-TBC1D1 was determined by the 14-3-3 overlay assay, and the co-precipitating endogenous 14-3-3s detected using the K19 antibody.

Figure 5 Relative contributions of phosphoSer237 and phosphoThr596 to 14-3-3 binding of HA-TBC1D1 in cells stimulated in different ways

HA-TBC1D1, the Thr596Ala and Ser237Ala single mutants, and Ser237Ala/Thr596Ala double mutant were immunoprecipitated from lysates of cells that had been stimulated as indicated, and analysed with the phosphospecific antibody that recognise phosphorylated Thr596. The co-precipitating endogenous 14-3-3s were detected using the K19 antibody. The same set of lysates were also analysed using the phospho-specific antibody that recognises phosphorylated Ser237. Anti-HA control blots are shown for each phospho-specific antibody blot.

Figure 6 Effects of protein kinase inhibitors on the multisite phosphorylation and 14-3-3 binding of TBC1D1 extracted from cells stimulated in different ways

A. HA-TBC1D1 proteins were immunoprecipitated using anti-HA antibody from lysates of transfected cells that were stimulated with IGF1 in the presence or absence of the PI3K inhibitor wortmannin, or with AMPK activators in the presence or absence of AMPK inhibitor Compound C (CC). Phosphorylation of HA-TBC1D1 was analysed using the phospho-specific antibodies that recognise phosphorylated Ser237 and Thr596. The 14-3-3 binding capacity of the HA-TBC1D1 was determined by the 14-3-3 overlay assay, and co-precipitating endogenous 14-3-3s detected using the K19 antibody.

B. HA-TBC1D1 was immunoprecipitated using anti-HA antibody from lysates of transfected cells that were stimulated with IGF1, EGF and PMA in the presence or absence of various kinase inhibitors (details in Materials and Methods). Phosphorylation of HA-TBC1D1 was analysed using the phospho-specific antibodies that recognise phosphorylated Ser237 and Thr596. The 14-3-3 binding capacity of the HA-TBC1D1 was determined by the co-precipitating endogenous 14-3-3s detected using the K19 antibody. For the bottom four panels, lysates (20 μg) were analysed with antibodies to monitor the phosphorylation status PKB, ACC and AMPK (pT308-PKB, pS79-ACC and pThr172-AMPK, respectively). Erk1/2 proteins act as the loading control.

Figure 7 In vitro phosphorylation of GST-TBC1D1 by PKB and AMPK

GST-TBC1D1 was expressed and purified from *E. coli*, and phosphorylated in vitro with PKB, and recombinant AMPK (rAMPK) and AMPK purified from rat liver. For the in vitro phosphorylations with two kinases, the sequential reactions were carried out through adding the enzymes in the order indicated (details in Materials and Methods). The phosphorylated proteins (300 ng per lane) were analysed by Western blots using anti-GST (A), anti-pSer237-TBC1D1 (B) and anti-pThr596-TBC1D1 (C) antibodies, and 14-3-3 overlay (D). The bottom panels in A and B are higher exposures that highlight the full-length GST-TBC1D1 protein (the faint band above the 150 kDa marker). The pThr596 antibody can only detect the GST-TBC1D1 at >150 and ~110 kDa, while the shorter forms are truncated from the C-terminus and (we presume) lack this residue.

Figure 8 Phosphorylation, 14-3-3-binding and subcellular localisation of endogenous TBC1D1 isolated from rat L6 myotubes

A. Endogenous TBC1D1 proteins were immunoprecipitated with anti-TBC1D1 antibody from lysates of rat L6 myotubes that were exposed to various stimuli (specified in Materials and Methods). WM is wortmannin. Phosphorylation of the endogenous TBC1D1 was analysed using the phospho-specific antibodies that recognise phosphorylated Ser237 and Thr596. The 14-3-3 binding capacity of the endogenous TBC1D1 was determined by the 14-3-3 overlay assay and co-precipitating endogenous 14-3-3s detected using the K19 antibody. For the bottom four panels, lysates (40 μg) were analysed with antibodies to monitor the phosphorylation status of acetyl CoA carboxylase (ACC), AMPK and PKB (pS79-ACC, pThr172-AMPK and pT308-PKB, respectively). Erk1/2 proteins represent the loading control.

B. Comparing the regulation of TBC1D1 and AS160. Similar to A, L6 myotubes were stimulated as indicated, endogenous TBC1D1 and AS160 were immunoprecipitated, and analysed by Western blotting and 14-3-3-overlay assay. Note that in addition to the full-length AS160 shown, the AS160 antibody detected a strong signal at >75 kDa (Supplementary Fig 4), which may represent a truncated form of the protein that lacks the N-terminal phosphorylated region.

C. Subcellular co-localisation of TBC1D1 and GluT4 in L6 myotubes. After differentiation for 4 days, L6 myotubes grown on glass coverslips were further cultured in serum-free medium for 4 h. The cells were left unstimulated, treated with insulin (100 nM for 30 min) or the AMPK activator A-769662 (50 μM for 1 h) as indicated. Cells were washed in PBS, fixed for 30 min in 4% paraformaldehyde in PBS, permeabilized with 0.2% Triton X-100 for 10 min, incubated in block solution (PBS buffer containing 0.2% Tween-20 and 3% BSA) for 15 min, rinsed in PBS and incubated with anti-TBC1D1 (Materials and Methods) and anti-GluT4 (Santa Cruz) antibodies in block solution for 1 h. After 3 x 10 min washes in PBS, cells were incubated with AlexaFluor-conjugated secondary antibodies (Invitrogen) for 1 h. After 3 x 10 min washes in PBS, slides were mounted with Hydromount (National Diagnostics), observed with a Leica confocal microscope, and representative images are shown. Controls experiments indicated that primary and secondary antibodies did not cross-react.

Biochemical Journal Immediate Publication. Published on 9 Nov 2007 as manuscript BJ20071114

Fig 1A

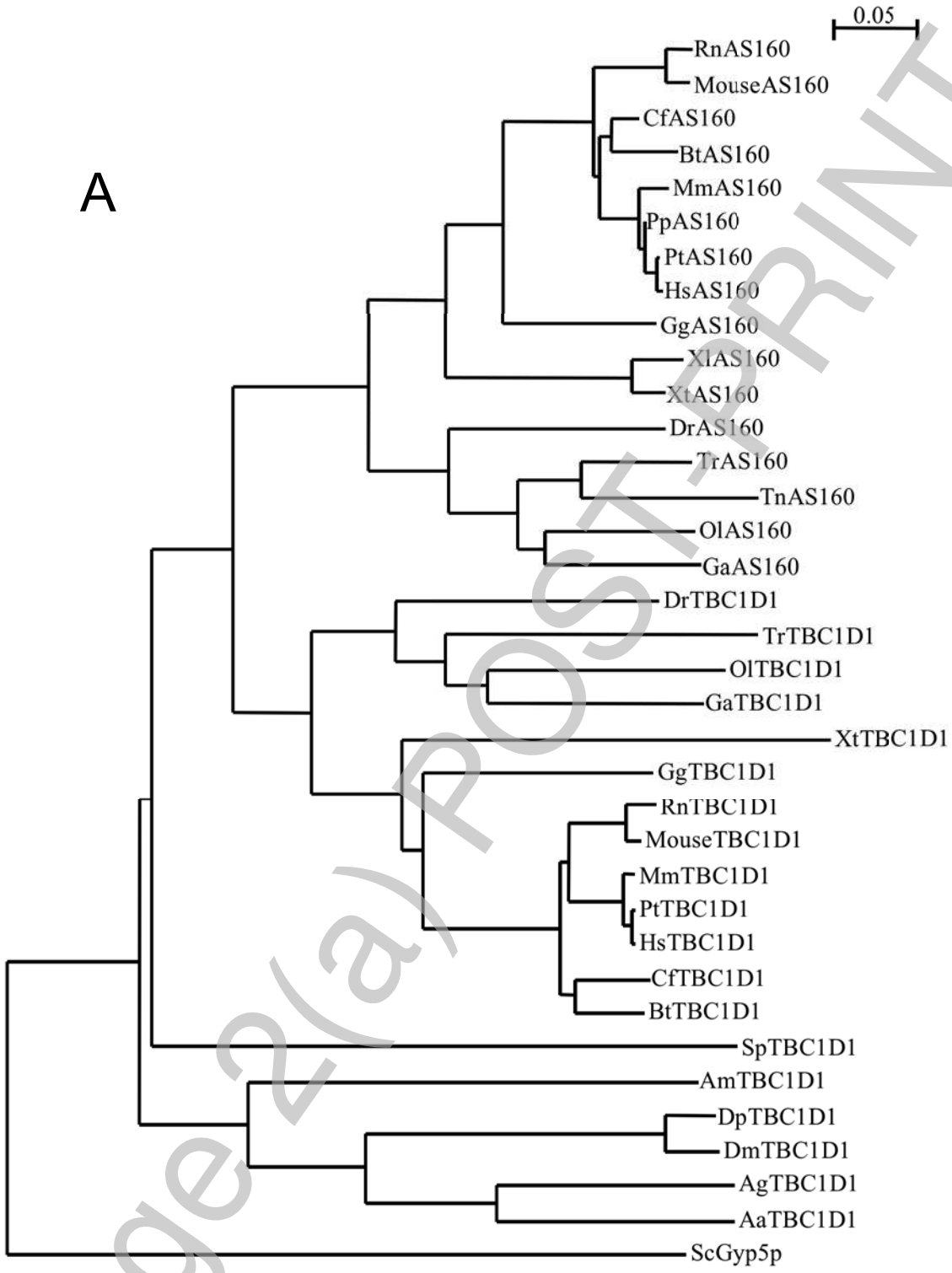

Biochemical Journal Immediate Publication. Published on 9 Nov 2007 as manuscript BJ20071114

Fig 1B

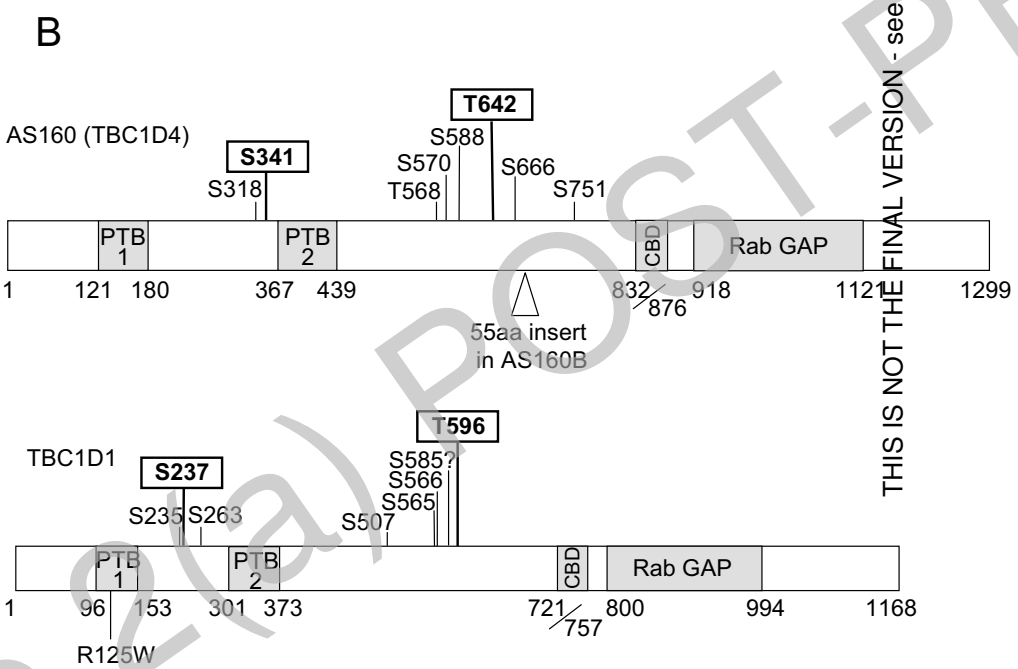

Biochemical Journal Immediate Publication. Published on 9 Nov 2007 as manuscript BJ20071114

Fig 1C

C

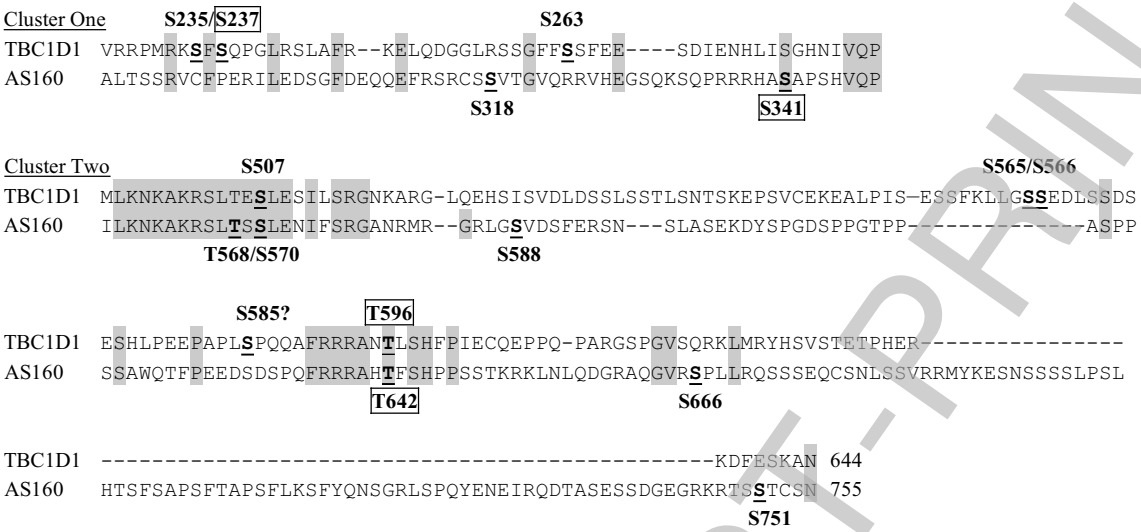

Biochemical Journal Immediate Publication. Published on 9 Nov 2007 as manuscript BJ20071114

Fig. 2 A-C

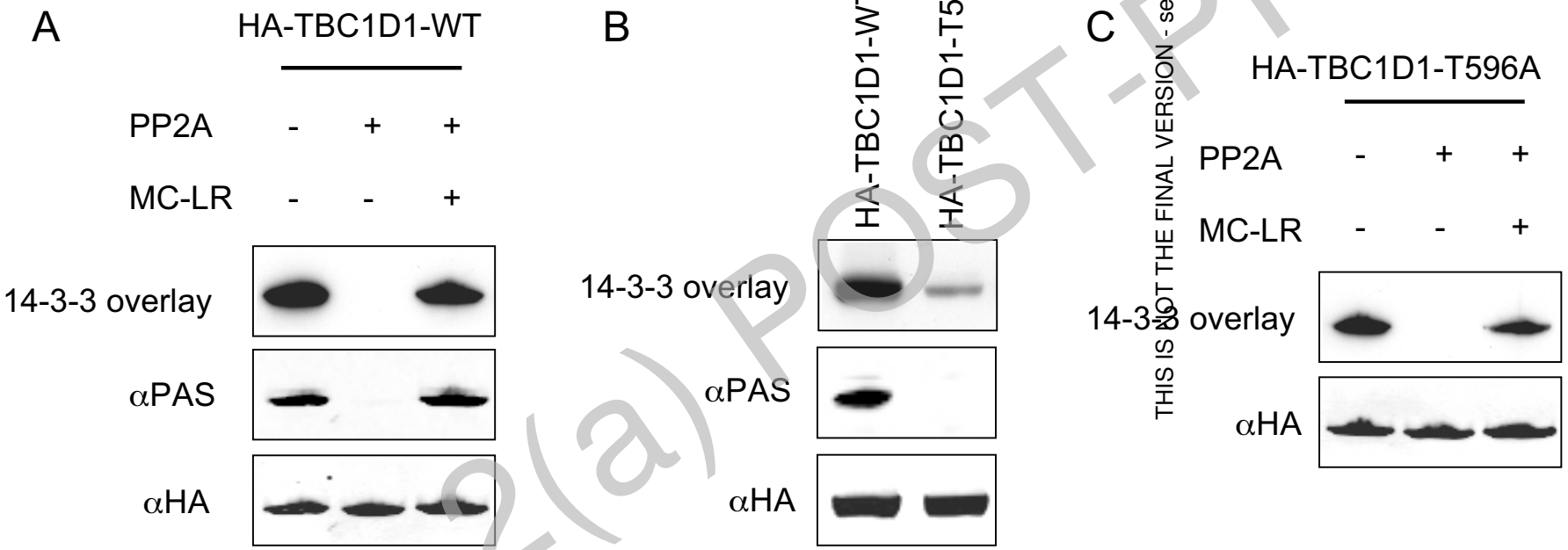

Biochemical Journal Immediate Publication. Published on 9 Nov 2007 as manuscript BJ20071114

Fig. 2 D

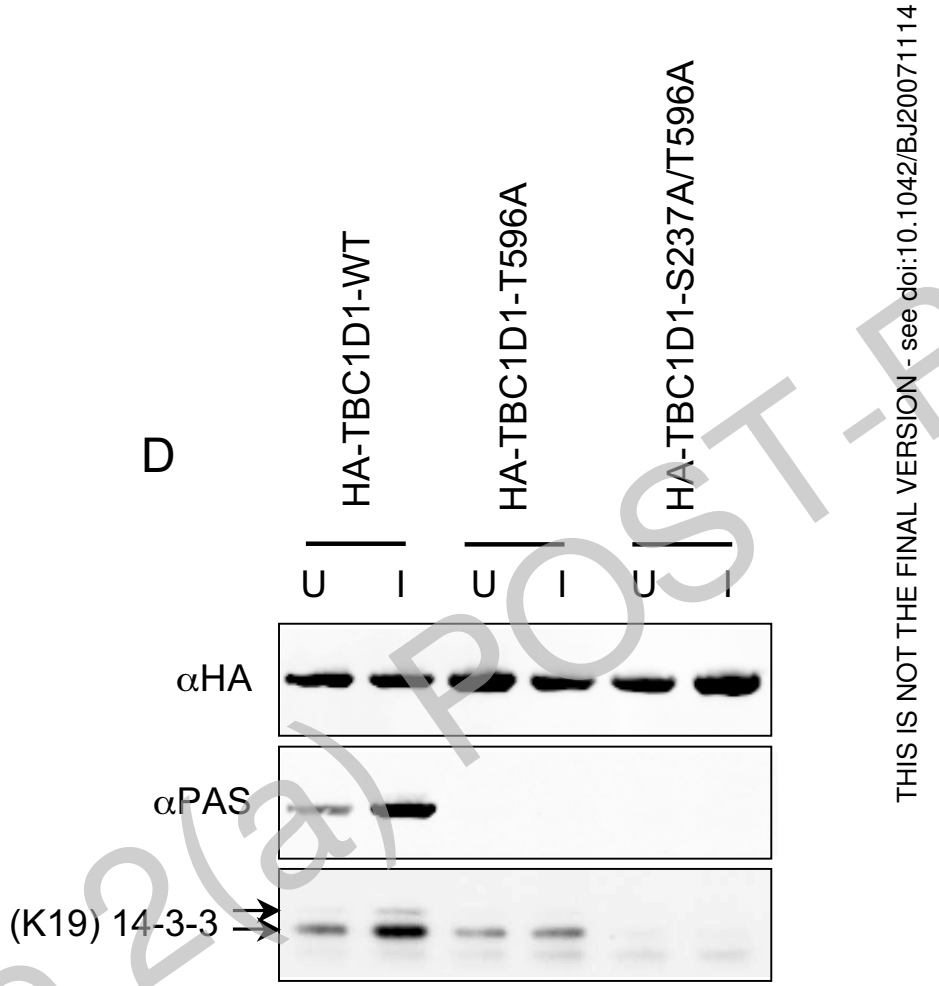

Biochemical Journal Immediate Publication. Published on 9 Nov 2007 as manuscript BJ20071114

Fig. 2 E

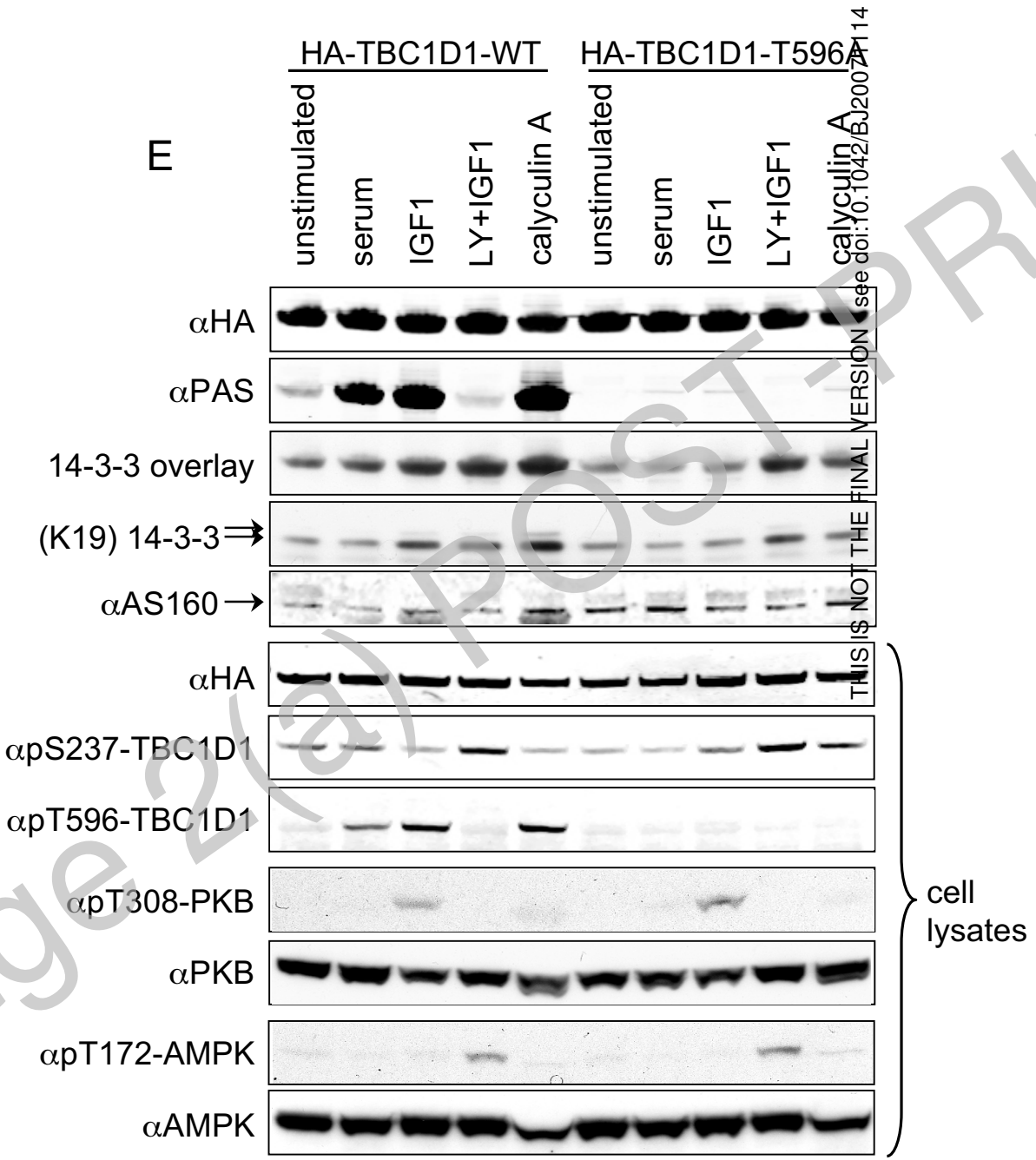

Fig. 3

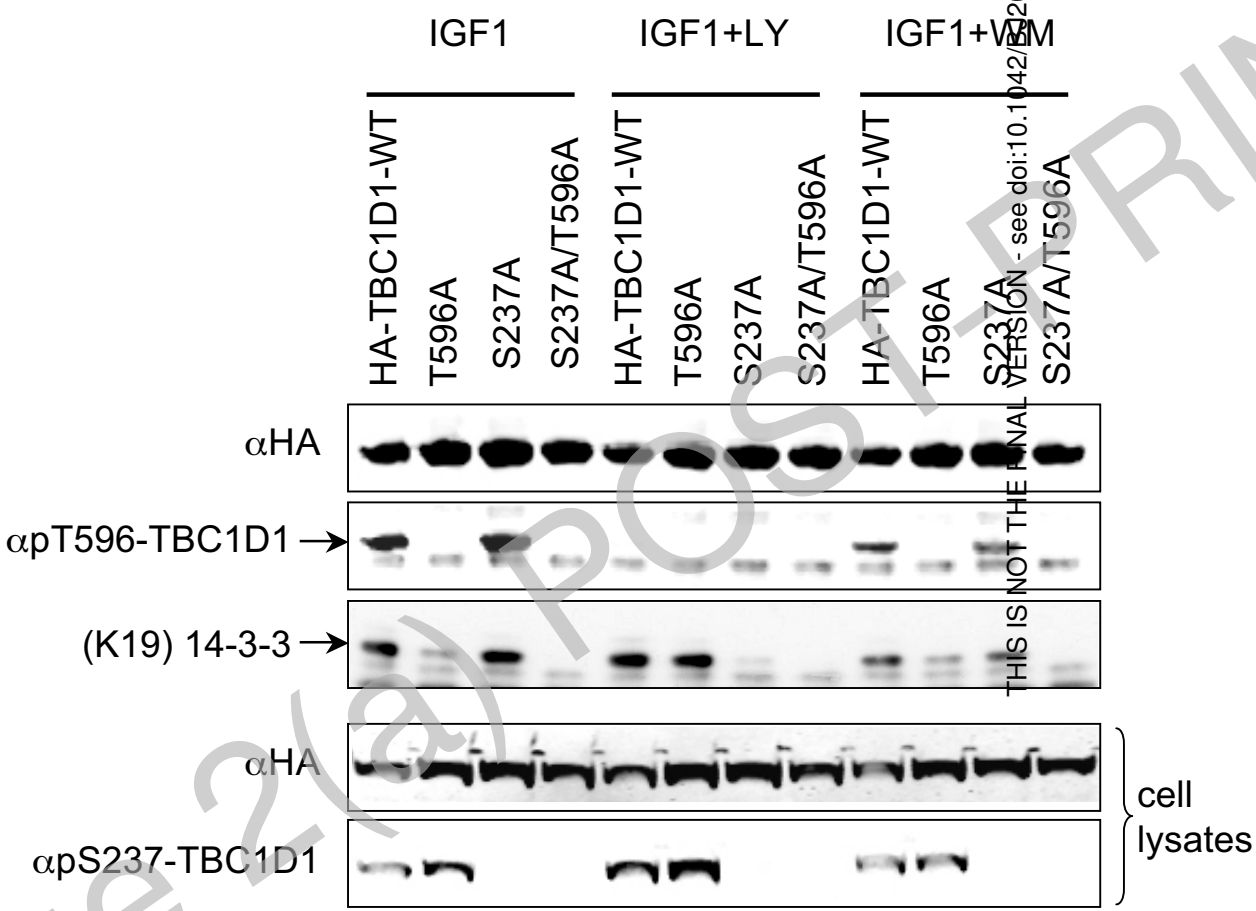

Fig. 4

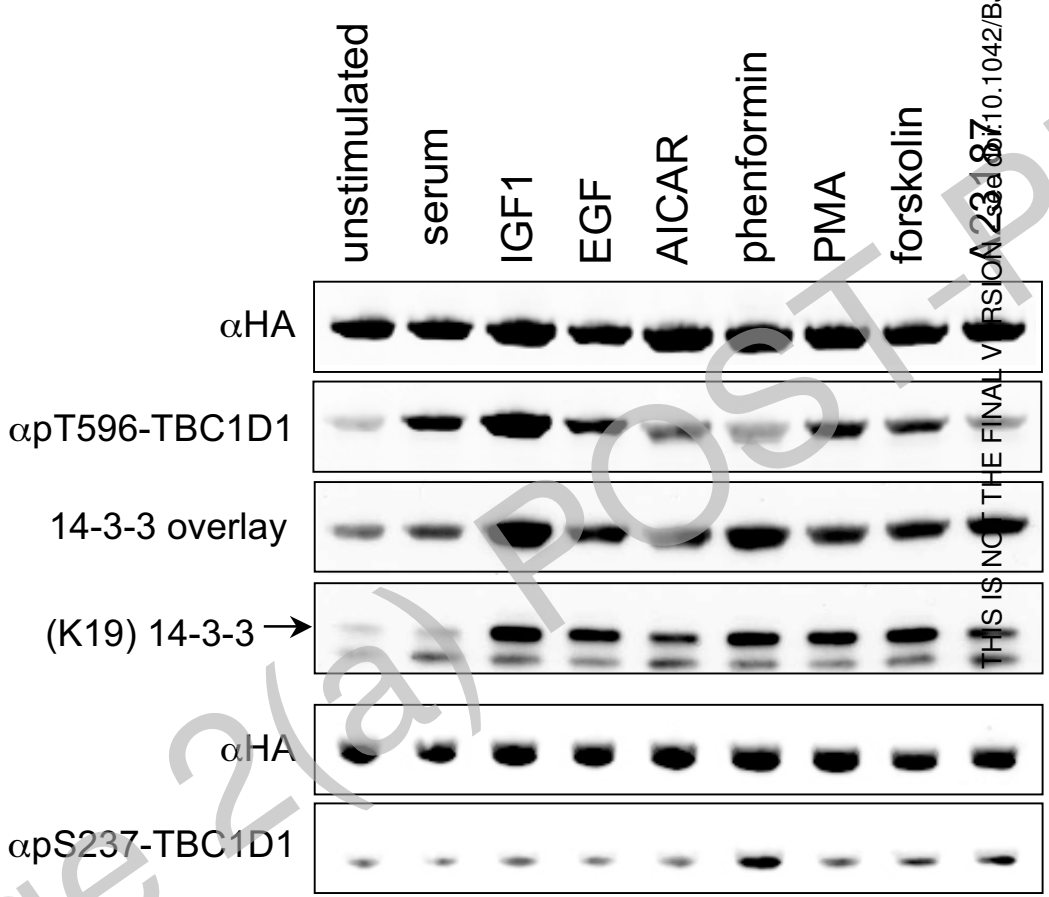

Fig. 5

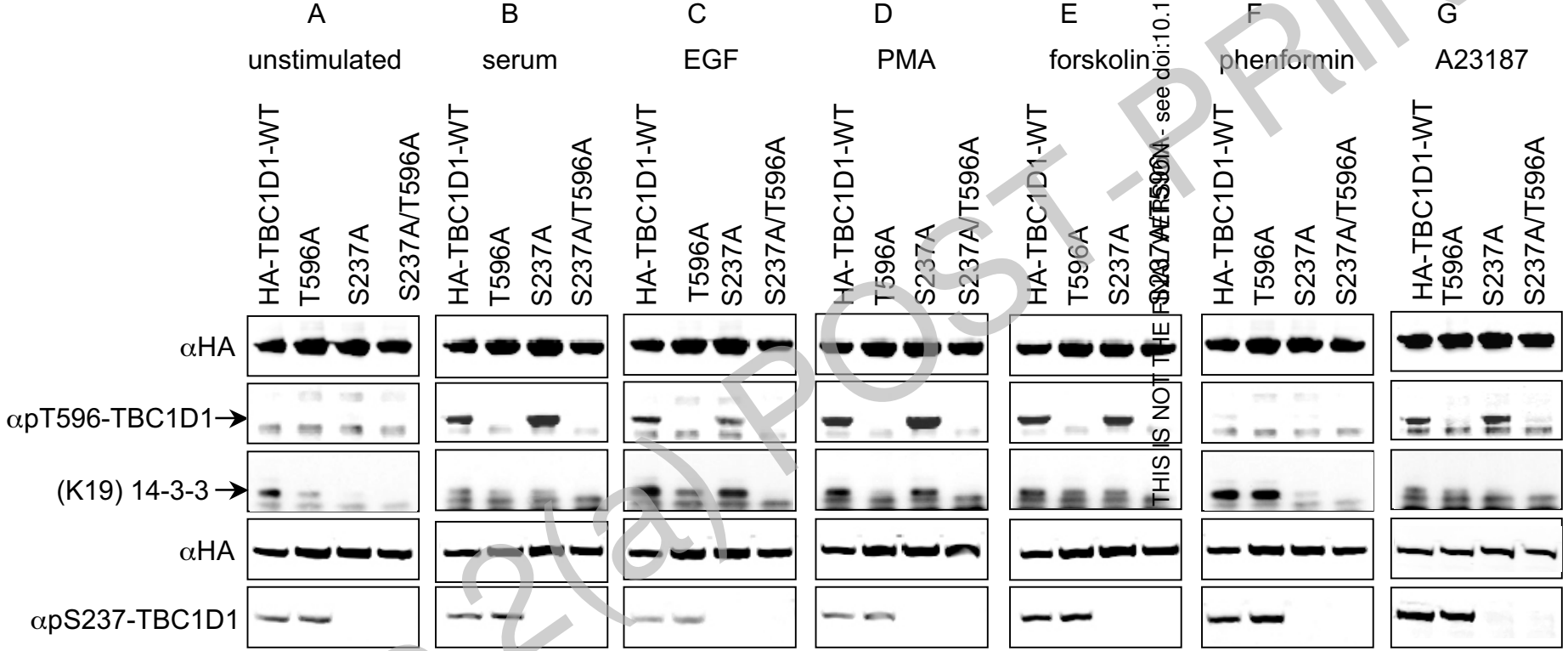

Biochemical Journal Immediate Publication. Published on 9 Nov 2007 as manuscript BJ20071114

Fig. 6A

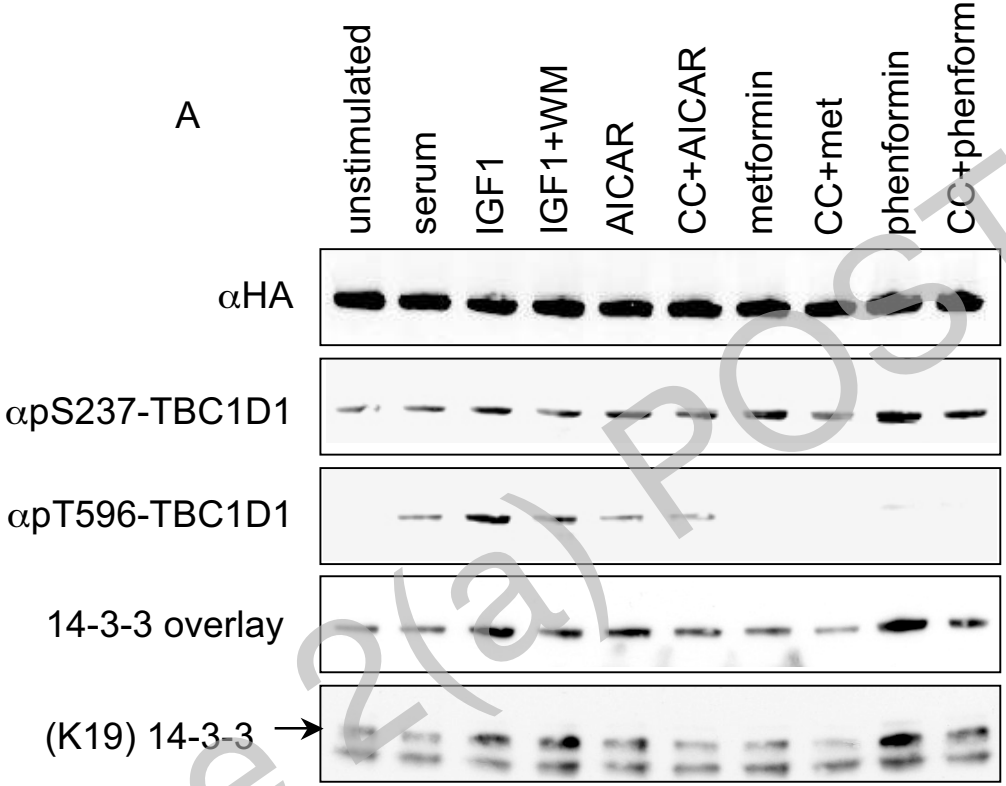

Biochemical Journal Immediate Publication. Published on 9 Nov 2007 as manuscript BJ20071114

Fig. 6B

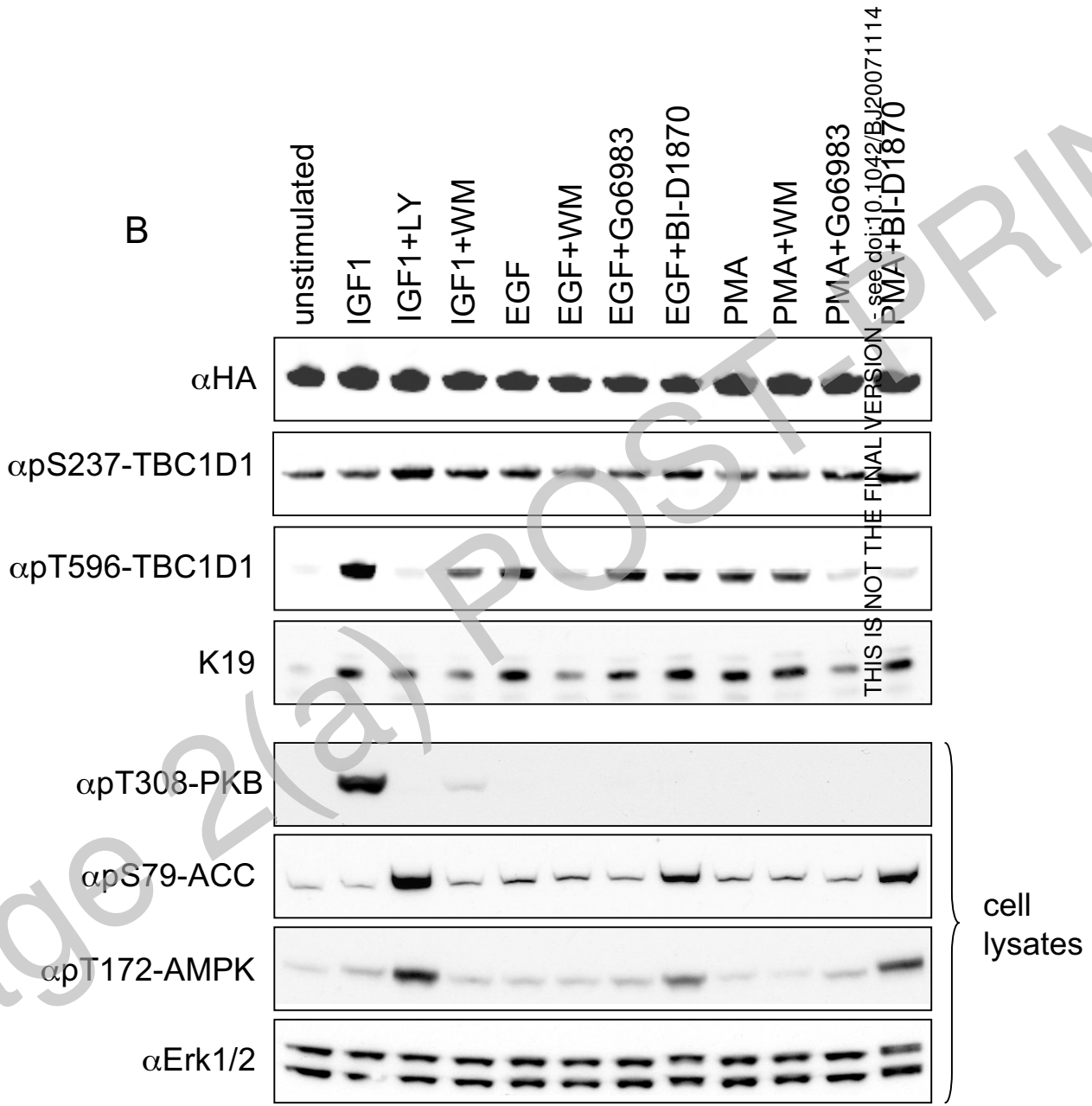

Biochemical Journal Immediate Publication. Published on 9 Nov 2007 as manuscript BJ20071114

Fig. 7

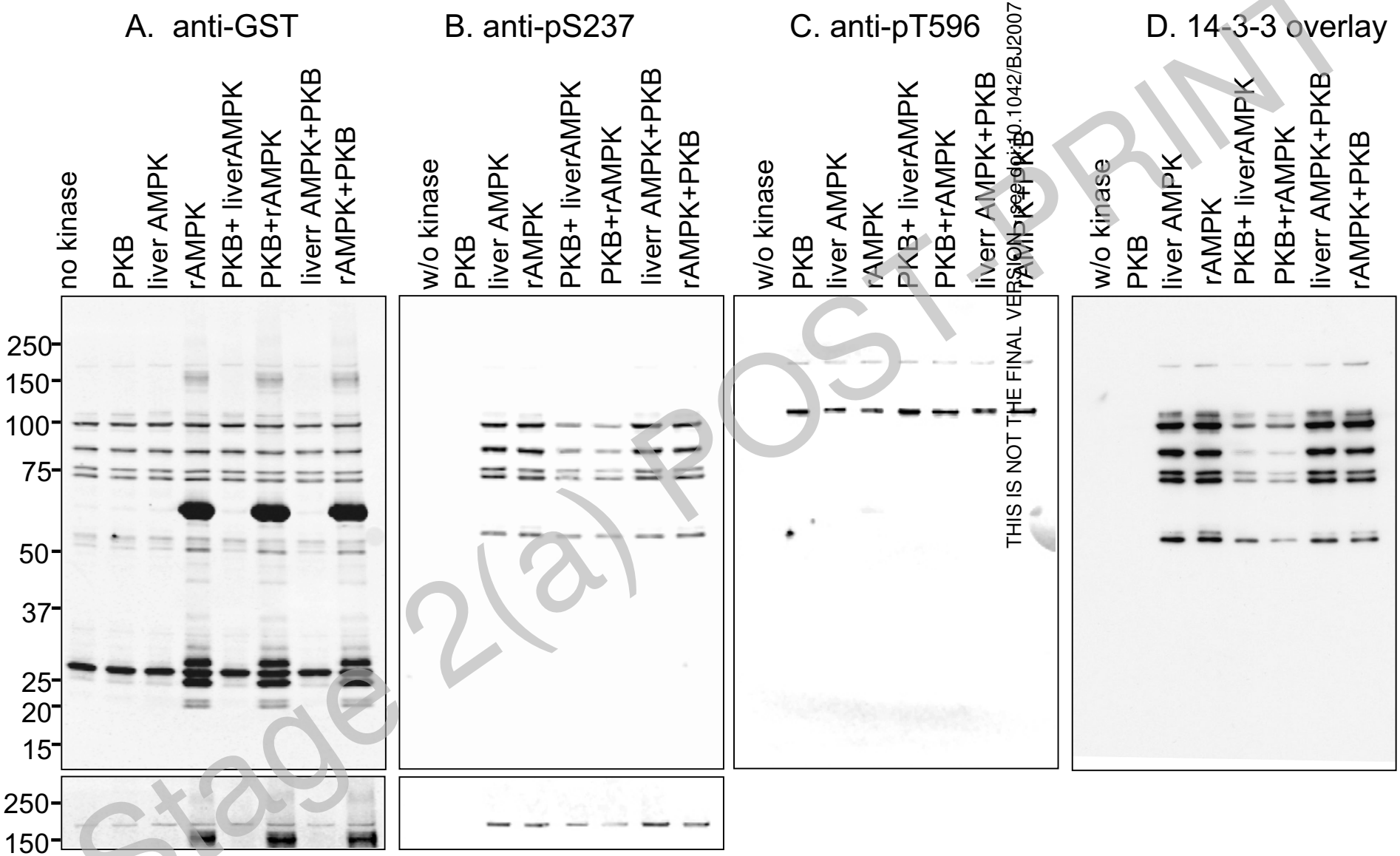

Biochemical Journal Immediate Publication. Published on 9 Nov 2007 as manuscript BJ20071114

Fig. 8A

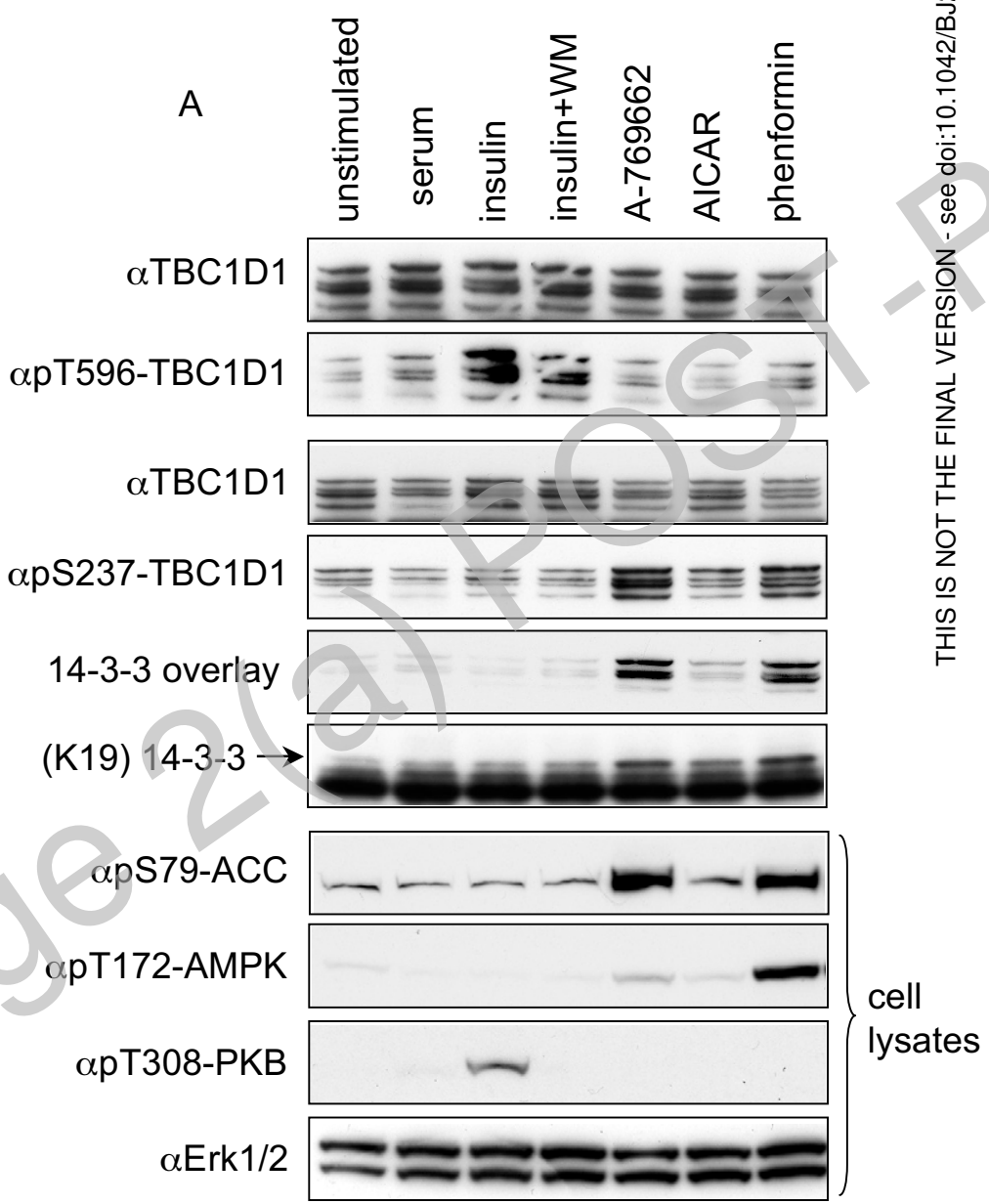

Biochemical Journal Immediate Publication. Published on 9 Nov 2007 as manuscript BJ20071114

Fig. 8B

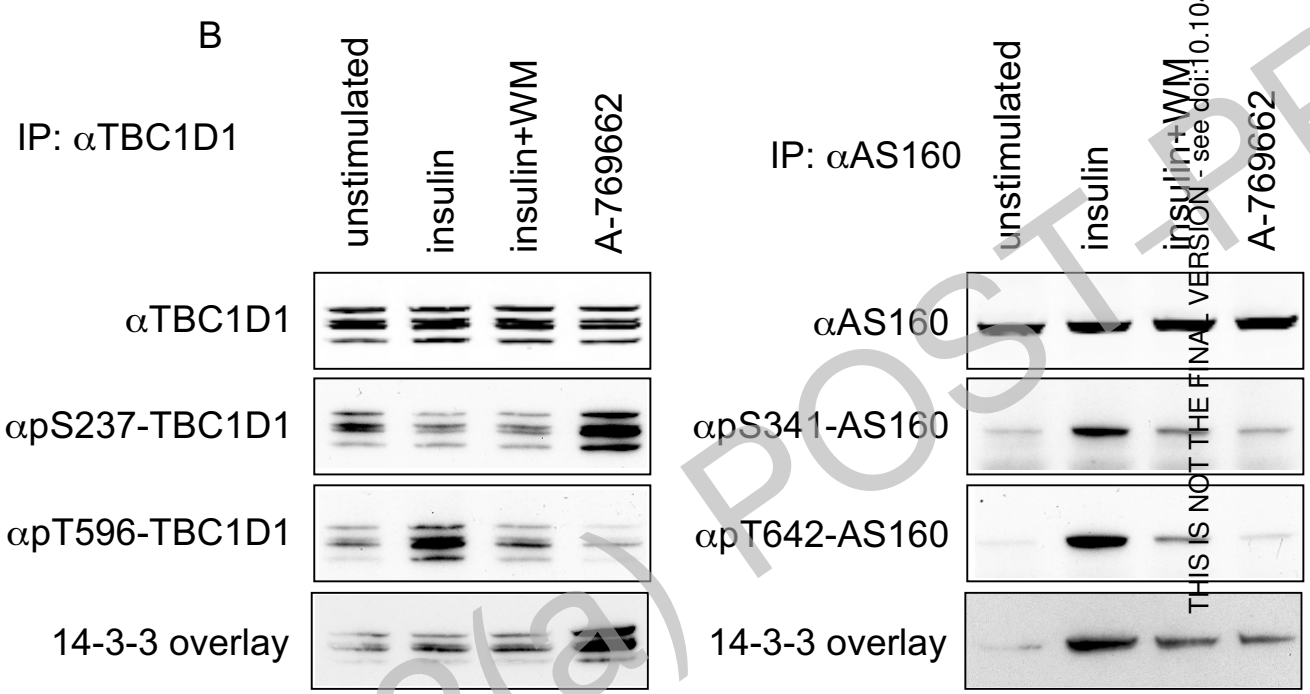

Biochemical Journal Immediate Publication. Published on 9 Nov 2007 as manuscript BJ20071114

Fig. 8C